

# Joint use of the Weniger transformation and hyperasymptotics for accurate asymptotic evaluations of a class of saddle-point integrals. II. Higher-order transformations

Riccardo Borghi

*Dipartimento di Elettronica Applicata, Università degli Studi “Roma Tre”*

*Via della Vasca Navale 84, I-00146 Rome, Italy*

## Abstract

The use of hyperasymptotics and the Weniger transformation has been proposed, in a joint fashion, for decoding the divergent asymptotic series generated by the steepest descent on a wide class of saddle-point integrals evaluated across Stokes sets [R. Borghi, Phys. Rev. E **78**, 026703 (2008)]. In the present sequel, the full development of the H-WT up to the second order in  $H$  is derived. Numerical experiments, carried out on several classes of saddle-point integrals, including the swallowtail diffraction catastrophe, show the effectiveness of the 2nd-level H-WT, in particular when the integrals are evaluated beyond the asymptotic realm.

PACS numbers: 02.60.Jh, 02.30.Lt, 02.60.-x, 02.70.-c, 02.30.Mv, 95.75.Pq

## I. INTRODUCTION

The present paper is a sequel of a previous work[1] concerning the evaluation of saddle-point integrals of the form

$$\mathcal{I}(k) = \int_{\mathcal{C}} g(s) \exp[-k f(s)] ds, \quad (1)$$

where  $\mathcal{C}$  is a suitable integration path in the complex  $s$ -plane,  $g(s)$  and  $f(s)$  are functions which, for simplicity, will be assumed to be nonsingular, and  $k$  will be intended as a “large” (in modulus) complex parameter. As is well known, the numerical evaluation of integrals of the kind in Eq. (1) is customarily required for solving several classes of physical problems, occurring in optics, quantum mechanics, statistical physics, fluid mechanics, and so on. In optics, the evaluation of several diffraction integrals is customarily carried out asymptotically by identifying the parameter  $k$  as the wavenumber of the radiation[2]. In quantum mechanics, the same role is played by the inverse of the Planck’s constant, while in fluid mechanics by the Reynold’s number[3].

In the stationary phase treatment of diffraction integrals the values of the associated complex wavefield are asymptotically evaluated by taking the contributions coming from the stationary points of  $f(s)$ , each of them associated to a “ray” in the corresponding geometrical picture. Of particular importance is the birth and the death, as the spatial parameters ruling the “phase” function  $if(s)$  vary, of “evanescent” rays across sets of codimension 1, named “Stokes sets” [4, 5].

The  $\delta$ -, or Weniger, transformation[6, 7, 8] (WT for short), is particularly efficient for resumming the factorial divergent asymptotic series well away from Stokes sets, as well as sets where two or more saddles are symmetrically placed in the complex singulant space[9]. Unfortunately, as with other resummation techniques[6, 10], the WT fails to perform across Stokes sets. The reason of such a failure stems to the extreme “specialization” of the transformation itself, which requires, for a successful resummation, an alternating sign pattern of the sequence of the single terms of the series[11]. Several methods have been conceived for resumming nonalternating, slowly convergent or divergent, sequences [8, 12], some of them being based on the serial combination of various resummation techniques[11, 13]. For the class of saddle-point integrals in Eq. (1), the marriage between hyperasymptotics[14, 15] (H for short) and the WT [1], generating the so-called H-WT (which stands for hyperasymptotic-Weniger transformation), allows the WT to successfully operate also across Stokes sets.

Basically, the H-WT consists in the sequential application, to the integral in Eq. (1), of a classical hyperasymptotic treatment, as described in Ref. [15], followed by the action of the WT on all asymptotic divergent series generated by H. In particular, the results obtained have shown how the 1st-order H-WT, for which only the first-stage of H is anticipated to the WT, is able to provide relative errors several orders of magnitude smaller than those achievable via the use of full hyperasymptotic treatments and with considerably lighter computational complexity and effort. A key aspect is that, differently from H, the first truncation operated on the starting asymptotic series has not to be an optimal, in the sense of superasymptotics (i.e., at the least term) one, but rather the corresponding truncation order, say  $N$ , must be used as a free parameter for the subsequent application of the WT.

A question which was not addressed in Ref. [1], but mentioned only in the last sentence, is whether WT and H can be combined to higher orders in H, and if so, how the accuracy improves with order. The present paper is aimed at giving a first answer to such a question. We shall limit our analysis only to the second stage of H. Further increasing of the H-WT order would be achievable along the same guidelines outlined here. On the other hand, it should be noted how, on increasing the order of H, the number of asymptotic series associated to the corresponding remainder that have to be resummed exponentially grows for topologies involving more than two saddles and, at the same time, the number of free parameters (i.e., the truncation orders at each H step) linearly increases. Accordingly, from a mere computational viewpoint, it is mandatory to find a compromise between the H-WT order and the computational effort. Some limits of the 1st-order H-WT have already been emphasized in Ref. [1], where asymptotic evaluations of saddle-point integrals for “small” values of the asymptotic parameter were considered. In such cases, in fact, to increase the parameter  $N$  of the 1st-order H-WT does not necessarily lead to an improvement of the reached accuracy, but often results in the opposite, i.e., a worsening of it. It is just the above scenario that we are interested in when the 2nd-level H-WT will be developed. Numerical experiments will be carried out on the class of saddle-point integrals already considered in the numerical sections of the first paper [1]. Moreover, asymptotic evaluations of the so-called swallowtail diffraction catastrophe [16] will be proposed as a new numerical experiment. The swallowtail function is defined via Eq. (1) with  $f(s)$  being a 5th-order polynomial with respect to  $s$ , thus involving a four saddle network. We will present a study of the accuracy achievable via H-WT asymptotic evaluations of the swallowtail diffraction

catastrophe for points placed at the Stokes set, following the prescriptions by Berry and Howls[5]. In doing so, we will find that the corresponding asymptotic expanding coefficients can be expressed in closed-form terms.

For any practical implementation of the H-WT, a key role is played by the numerical evaluation of the corresponding hyperterminants[14, 15] which are defined through suitable multiple integrals. For the lowest-order hyperterminant the exact analytical expression is available from literature[14], but unfortunately this is not true for higher-order hyperterminants, included those involved in the 2nd-level H-WT. In the present paper we solve the problem of the 2nd-level hyperterminant exact evaluation for a particular, but very important, choice of the hyperterminant parameters, which often occurs in the implementation of H for evaluating a wide class of saddle-point integrals. Up to our knowledge, this is a new result which also provides an interesting connection of such hyperterminants to the Meijer-G functions [17]. Moreover, although the closed-form evaluation of 2nd-level hyperterminants for arbitrary choices of their parameters seems to remain an open problem, in the present paper we find a semi-analytical representation which turns out to be suitable for numerical calculations via standard integration packages. Similarly as done in Ref. [1], one of our aims is to keep the paper reasonably self-consistent. Accordingly, in the next section a brief review of H, up to the 2nd-level, is given. As far as the WT is concerned, we believe that what is contained in Ref. [1], together with the extensive bibliography, should be enough also for a nonexpert reader. For this reason, we do not repeat it in the present paper.

## II. RESUMING HYPERASYMPTOTICS

### A. Preliminaries and notations

For simplicity, we shall refer to the asymptotic evaluation of saddle-point integrals of the type in Eq. (1) where the set of saddle points of  $f(s)$  will be denoted  $\mathcal{S}$  and the integration path  $\mathcal{C}$  will be thought of as the union of a finite number of steepest descent arcs each of them, say  $\mathcal{C}_n$ , passing through the contributive saddle point  $s_n$ , which will be supposed to be a simple one. Accordingly, the quantity  $\mathcal{I}(k)$  can generally be written as

$$\mathcal{I}(k) = \int_{\mathcal{C}} g(s) \exp[-k f(s)] ds = \sum_{n \in \mathcal{S}'} \mathcal{I}^{(n)}(k), \quad (2)$$

where  $\mathcal{S}'$  denotes the subset of  $\mathcal{S}$  containing all the contributive saddles, and

$$\mathcal{I}^{(n)}(k) = \int_{\mathcal{C}_n} g(s) \exp[-kf(s)] ds. \quad (3)$$

The last integral can be written as[15]

$$\mathcal{I}_n(k) = k^{-1/2} \exp(-kf_n) T^{(n)}(k), \quad (4)$$

where  $f_n = f(s_n)$ , and where  $T^{(n)}(k)$  can *formally* be written through the following asymptotic series expansion:

$$T^{(n)}(k) = \sum_{r=0}^{\infty} k^{-r} T_r^{(n)}, \quad (5)$$

the expanding coefficients  $T_r^{(n)}$  being expressed via the integral representation [15]

$$T_r^{(n)} = \frac{(r-1/2)!}{2\pi i} \oint_n \frac{g(s)}{[f(s) - f_n]^{r+1/2}} ds, \quad (6)$$

where the subscript  $n$  denotes a small positive loop around the saddle  $s_n$ .

## B. Development of H up to the second stage

H starts by writing Eq. (5) in the form

$$T^{(n)}(k) = \sum_{r=0}^{N-1} k^{-r} T_r^{(n)} + R^{(n)}(k, N), \quad (7)$$

where  $N$  represents a positive integer and  $R^{(n)}(k, N) = \sum_{r=N}^{\infty} k^{-r} T_r^{(n)}$ , denotes the corresponding remainder which, due to the diverging character of the asymptotic series, turns out to be a *diverging* quantity too. H is based on a couple of fundamental results, found via a nontrivial analysis in Ref. [15]. The first is that the value of the expanding coefficients  $T_r^{(n)}$  at the saddle  $s_n$  is strictly related to the values of the expanding coefficients  $T_r^{(m)}$  at all those saddles, say  $\{s_m\}$ , which are *adjacent* to  $s_n$ , via the following formal resurgence relation[15]:

$$T_r^{(n)} = \frac{1}{2\pi i} \sum_{m \in \mathcal{A}_n} (-1)^{\gamma_{nm}} \sum_{l=0}^{\infty} \frac{(r-l-1)!}{F_{nm}^{r-l}} T_l^{(m)}, \quad (8)$$

where  $\mathcal{A}_n$  denotes the set containing the indexes pertinent to all saddles adjacent to  $s_n$ , the quantities  $F_{nm}$ , called *singulants*, are defined by

$$F_{nm} = f_m - f_n, \quad (9)$$

and the binary quantities  $\gamma_{nm} \in \{0, 1\}$  are obtained through a topological rule[15]. The other fundamental tool of H is the following integral representation of the remainder  $R^{(n)}(k, N)$ [15]:

$$R^{(n)}(k, N) = \frac{1}{2\pi i} \sum_{m \in \mathcal{A}_n} \frac{(-1)^{\gamma_{nm}}}{(kF_{nm})^N} \times \int_0^\infty dv \frac{v^{N-1} \exp(-v)}{1 - \frac{v}{kF_{nm}}} T^{(m)} \left( \frac{v}{F_{nm}} \right). \quad (10)$$

Equations (5)-(10) allow hyperasymptotic expansions for the saddle integral in Eq. (3) to be built up in principle to any order[15]. For instance, the direct substitution of Eq. (5) into Eq. (10) leads to the 1st-stage hyperasymptotic expansion [1],

$$T^{(n)}(k) = \sum_{r=0}^{N-1} k^{-r} T_r^{(n)} + \frac{(-1)^N}{2\pi i} \sum_{m \in \mathcal{A}_n} (-1)^{\gamma_{nm}} \times \sum_{r=0}^{\infty} (-1)^r k^{-r} T_r^{(m)} K_{N-r}^{(1)}(-kF_{nm}), \quad (11)$$

where the function  $K_n^{(1)}(\beta)$ , called *hyperterminant* of order 1[14, 15], is defined through the integral

$$K_n^{(1)}(\beta) = \frac{1}{\beta^n} \int_0^\infty dv \frac{v^{n-1} \exp(-v)}{1 + \frac{v}{\beta}}, \quad (12)$$

where, in order for it to converge,  $n > 0$ . Moreover, it can be shown that[1]

$$K_n^{(1)}(\beta) = \exp(\beta) \frac{E_n(\beta)}{\beta^{n-1}} (n-1)! + (-1)^{n-1} i\pi\epsilon \exp(\beta), \quad (13)$$

where  $E_n(\cdot)$  denotes the exponential integral function [17], while  $\epsilon$  equals 1 if  $\beta < 0$  and zero otherwise. The presence of the term containing  $\epsilon$  has to be ascribed to the evaluation of the integral in Eq. (12), when  $\beta < 0$ , in the Cauchy principal-value sense. Equation (11) represents the first hyperasymptotic stage, at which the divergence of the asymptotic series in Eq. (5) is led back to the presence of adjacent saddles [15]. Furthermore, the asymptotic series in Eq. (11) are only formal, since for  $r > N$  the terminant  $K_{N-r}^{(1)}$  diverges. In Ref. [1] Eq. (11) was taken as the starting point for introducing the H-WT. In particular, instead

of using the WT directly on the single terms of the series in Eq. (5), it is employed for resumming the asymptotic series associated to all saddles  $s_m$ , with  $m \in \mathcal{A}_n$ , which appear in Eq. (11). Of course, due to the fact that  $r \leq N$  in Eq. (11), it is mandatory that  $N$  be left as a free parameter, in order for the WT to be able in decoding the above asymptotic series. The 2nd-level H can be derived by truncating each of the asymptotic series in Eq. (11) at an order, say  $M$ , and by generating, for *each* adjacent saddle  $s_m$ , with  $m \in \mathcal{A}_n$ , a list of asymptotic series associated to all saddles, say  $s_h$ , such that  $h \in \mathcal{A}_m$ . In Appendix A, only for the reader convenience, the derivation of the 2nd-level hyperasymptotic expansion of the integral in Eq. (1) is briefly recalled according to the formalism of Ref. [15]. In particular, it is found that

$$\begin{aligned}
T^{(n)}(k) &= \sum_{r=0}^{N-1} k^{-r} T_r^{(n)} \\
&+ \frac{(-1)^N}{2\pi i} \sum_{m \in \mathcal{A}_n} (-1)^{\gamma_{nm}} \\
&\times \sum_{r=0}^{M-1} (-1)^r k^{-r} T_r^{(m)} K_{N-r}^{(1)}(-kF_{nm}) \\
&+ \frac{(-1)^{N+M}}{(2\pi i)^2} \sum_{m \in \mathcal{A}_n} \sum_{h \in \mathcal{A}_m} (-1)^{\gamma_{nm} + \gamma_{mh}} \\
&\times \sum_{r=0}^{\infty} k^{-r} T_r^{(h)} K_{M-r, N-M}^{(2)}\left(-kF_{nm}; -\frac{F_{mh}}{F_{nm}}\right),
\end{aligned} \tag{14}$$

where  $K_{n,m}^{(2)}(\beta; \gamma)$ , the hyperterminant of order 2, is now defined through the double integral

$$\begin{aligned}
K_{n,m}^{(2)}(\beta; \gamma) &= \frac{1}{\beta^{n+m}} \\
&\times \int_0^\infty \int_0^\infty du dv \exp(-u - \gamma v) \frac{u^{m-1} v^{n-1}}{\left(1 + \frac{u}{\beta}\right) \left(1 + \frac{v}{u}\right)}.
\end{aligned} \tag{15}$$

Similarly as we done in Ref. [1], Eq. (14) can be used to give estimates of  $T^{(n)}(k)$ , as functions of the two (free) parameters  $N$  and  $M$ , by resumming, via the WT, all asymptotic series generated at the second stage of H which are inside the double sum with respect to  $h$  and  $m$ .

### III. ON THE EVALUATION OF $K_{n,m}^{(2)}(\beta; \gamma)$

The numerical evaluation of the hyperterminants represents a step of fundamental importance for any practical implementation of the H-WT algorithm. Unfortunately, differently from the lowest-order H-WT, for which the corresponding hyperterminants are achievable via the closed-form expression in Eq. (13), there are no analytical expressions available for higher-order hyperterminants. In a series of important papers, Olde Daalhuis [18, 19] addressed the general problem of the hyperterminants evaluation, up to arbitrary precisions, through the use of convergent series representations based on hypergeometric functions. However, for the particular case of the 2nd-level hyperterminant, it seems that some new, at least up to our knowledge, results could be established.

From Eq. (15) where, in order for it to converge,  $n > 0$  and  $m > 0$ , the hyperterminant can be written as

$$K_{n,m}^{(2)}(\beta; \gamma) = \frac{1}{\beta^{n+m}} \times \int_0^\infty \int_0^\infty du dv \exp(-u - \gamma v) \frac{u^m v^{n-1}}{\left(1 + \frac{u}{\beta}\right) (u + v)}, \quad (16)$$

and, by formally expanding the factor  $1/(1 + u/\beta)$  as a geometric series, after some algebra takes the form

$$\begin{aligned} K_{n,m}^{(2)}(\beta; \gamma) &= \frac{(-1)^m}{\beta^n} \sum_{k=m}^\infty \left(-\frac{1}{\beta}\right)^k \\ &\times \int_0^\infty \int_0^\infty du dv \exp(-u - \gamma v) \frac{u^k v^{n-1}}{u + v} = \\ &= (-1)^m \frac{(n-1)!}{(\beta\gamma)^n} \\ &\times \sum_{k=m}^\infty \left(-\frac{1}{\beta}\right)^k \frac{k!}{k+n} F\left(n, 1; k+n+1; 1 - \frac{1}{\gamma}\right), \end{aligned} \quad (17)$$

where  $F(\cdot, \cdot; \cdot; \cdot)$  denotes the hypergeometric function[17]. Although the series in Eq. (17) is divergent, it can be decoded via Borel summation, i.e., by replacing the term  $k!$  by its



integral representation, i.e.,

$$k! = \int_0^\infty dt \exp(-t) t^k, \quad (18)$$

which, once substituted into Eq. (17), leads to

$$\begin{aligned} K_{n,m}^{(2)}(\beta; \gamma) &= (-1)^m \frac{(n-1)!}{(\beta\gamma)^n} \int_0^\infty dt \exp(-t) \\ &\times \sum_{k=m}^\infty \left(-\frac{t}{\beta}\right)^k \frac{1}{k+n} F\left(n, 1; k+n+1; 1-\frac{1}{\gamma}\right). \end{aligned} \quad (19)$$

Although, as we shall in a moment, it is possible to express the series inside the last equation through a closed form, it is better to carry out the evaluations for the case  $\gamma = 1$  and  $\gamma \neq 1$  separately.

On letting into Eq. (19)  $\gamma = 1$  we have

$$\begin{aligned} K_{n,m}^{(2)}(\beta; 1) &= (-1)^m \frac{(n-1)!}{\beta^n} \\ &\times \int_0^\infty dt \exp(-t) \sum_{k=m}^\infty \left(-\frac{t}{\beta}\right)^k \frac{1}{k+n} = \\ &= \frac{(n-1)!}{(m+n)\beta^{n-1}} \\ &\times \int_0^\infty dt \exp(-t) \left(\frac{t}{\beta}\right)^m F\left(m+n, 1; m+n+1; -\frac{t}{\beta}\right). \end{aligned} \quad (20)$$

The integral in Eq. (20) can be evaluated by using the representation of the hypergeometric function given by formula 9.34.7 of Ref. [17]. In particular, it turns out that

$$\begin{aligned} K_{n,m}^{(2)}(\beta; 1) &= \frac{(n-1)!}{\beta^{n-1}} \\ &\times \int_0^\infty dt \exp(-t) \left(\frac{t}{\beta}\right)^{m+1} G_{22}^{12} \left( \frac{t}{\beta} \left| \begin{matrix} -n-m, -1 \\ -1, -n-m-1 \end{matrix} \right. \right), \end{aligned} \quad (21)$$

where  $G_{pq}^{mn}(\cdot)$  denotes the Meijer function[17]. Finally, by using formulas 9.31.5, 7.813.1, and 9.31.2 of [17], after some algebra it is found that

$$K_{n,m}^{(2)}(\beta; 1) = (n-1)! G_{23}^{31} \left( \beta \left| \begin{matrix} 1-n-m, 1 \\ 1-n, 1-n-m, 0 \end{matrix} \right. \right). \quad (22)$$

Equation (22) represents one of the main results of the present paper. As we shall see in the numerical section, in applying the 2nd-level H-WT the evaluation of the hyperterminants  $K_{n,m}^{(2)}(\beta; \gamma)$  is often required for  $\gamma = 1$ . This happens whenever the contributive saddle  $s_n$  turns out to be adjacent to itself after two hyperasymptotic stages, i.e., when  $h = n$  into Eq. (14)[15].

For  $\gamma \neq 1$ , the series inside the integral in Eq. (17) can still be expressed through a closed form, although the subsequent integral unfortunately not. However, a semi-analytical expression, which turns out to be suitable for being evaluated via standard numerical integration packages can be derived. In doing this, Eq. (17) is first rewritten as

$$K_{n,m}^{(2)}(\beta; \gamma) = (-1)^m \frac{(n-1)!}{(\beta\gamma)^n} \times \left[ \mathcal{S} - \sum_{k=0}^{m-1} \left( -\frac{1}{\beta} \right)^k \frac{k!}{k+n} F \left( n, 1; k+n+1; \frac{\gamma-1}{\gamma} \right) \right], \quad (23)$$

where

$$\mathcal{S} = \sum_{k=0}^{\infty} \left( -\frac{1}{\beta} \right)^k \frac{k!}{k+n} F \left( n, 1; k+n+1; \frac{\gamma-1}{\gamma} \right), \quad (24)$$

so that the task is to evaluate the series in Eq. (24) for  $\gamma \neq 1$ . On substituting from Eq. (18) into Eq. (24) we have

$$\begin{aligned} \mathcal{S} &= \int_0^{\infty} dt \exp(-t) \\ &\times \sum_{k=0}^{\infty} \left( -\frac{t}{\beta} \right)^k \frac{F \left( n, 1; k+n+1; 1 - \frac{1}{\gamma} \right)}{k+n} = \\ &= \gamma \int_0^{\infty} dt \exp(-t) \\ &\times \sum_{k=0}^{\infty} \left( -\frac{t}{\beta} \right)^k \frac{F(1+k, 1; n+1+k; 1-\gamma)}{k+n}, \end{aligned} \quad (25)$$

where use has been made of the relation[see Ref. [20] p. 347]

$$F \left( n, 1; k+n+1; 1 - \frac{1}{\gamma} \right) = \gamma F(1+k, 1; n+1+k; 1-\gamma). \quad (26)$$

Finally, on writing Eq. (25) as

$$\begin{aligned} \mathcal{S} &= \frac{\gamma}{n} \int_0^\infty dt \exp(-t) \\ &\times \sum_{k=0}^\infty \frac{(1)_k}{k!} \frac{(n)_k}{(n+1)_k} \left(-\frac{t}{\beta}\right)^k F(1+k, 1; n+1+k; 1-\gamma), \end{aligned} \quad (27)$$

where  $(\cdot)_k$  denotes the Pochhammer symbol, formula 6.7.1.8 of Ref. [20] gives at once

$$\mathcal{S} = \frac{\gamma}{n} \int_0^\infty dt \frac{\exp(-t)}{1 + \frac{t}{\beta}} F\left(1, 1; n+1; 1 - \frac{\gamma}{1 + \frac{t}{\beta}}\right). \quad (28)$$

Notice that, when  $\text{Re}[\beta] > 0$ , the function  $S$  can also be evaluated through the alternative form

$$\mathcal{S} = \frac{\beta\gamma}{n} \int_0^1 dp \frac{\exp\left[-\beta\left(\frac{1}{p} - 1\right)\right]}{p} F(1, 1; n+1; 1 - \gamma p). \quad (29)$$

Although it seems that the above expressions cannot be further simplified, the numerical evaluation of the function  $S$  can be done with high accuracies by using standard integration packages. Finally, it should be stressed that, for  $\beta < 0$ , the evaluation of the double integral defining  $K_{n,m}^{(2)}(\beta; \gamma)$  has to be done, with respect to the  $v$ -variable, in the Cauchy principal value sense, in order to overcome the singularity placed at  $v = -\beta$ . This, in turn, implies that an extra term must be added to the result. In Appendix B such term is analytically evaluated starting from the definition in Eq. (15), and turns out to be

$$i\pi (-1)^{n+m-1} (n-1)! \frac{\exp[\beta(1-\gamma)]}{(-\beta)^{n-1}} E_n(-\beta\gamma). \quad (30)$$

All subsequent numerical experiments will be done within the *Mathematica* language.

## IV. NUMERICAL EXPERIMENTS

### A. Evaluation of the Airy function across the Stokes line

Consider the evaluation of the Airy function, defined as

$$\text{Ai}(x) = \frac{1}{2\pi} \int_{\mathcal{C}} \exp\left[i\left(\frac{s^3}{3} + xs\right)\right] ds, \quad (31)$$

which is of the form given in Eq. (1) with  $g(s) = 1/(2\pi)$ ,  $f(s) = -i(s^3/3 + xs)$ , and  $k = 1$ . The detailed analysis of the saddle topology, as well as the expanding coefficients  $T_r^{(n)}$  has been summarized in Ref. [1], so that here it will not be given again. We only recall that the two saddles are  $s_1 = (-x)^{1/2}$  and  $s_2 = -s_1$ , and that  $\mathcal{A}_2 = \{^2_1\}$ ,  $\gamma_{12} = 0$ ,  $\gamma_{21} = 1$ . We focus our attention on the evaluation of the Airy function across the Stokes line[21], i.e., for  $\arg\{x\} = 2\pi/3$ , in order to compare the performances of the 2nd-level H-WT with respect those displayed by the 1st-order H-WT in the same situation. More precisely, we write the argument of the Airy function as  $x = (3/4 \times F)^{2/3} \exp(i2\pi/3)$ , where  $F$  is a real positive parameter, whose value coincides with the singulant  $F_{12}$ . The study of the asymptotic evaluation of the Airy function across its Stokes line has played a pivotal role in the development of several asymptotic technique, mainly in light of the relative simplicity of the involved saddle topology. Such a simplicity could help in grasping, whereas possible, some conceptual aspects related to the use of the H-WT. Differently from what done in Ref. [1], where the relative error values were displayed via the use of tables, in the present paper we are going to resort to graphical visualizations, due to the presence of the two “free” parameters  $N$  and  $M$ . In the first experiment, whose results are shown in Figure 1, the Airy function is evaluated for  $F = 16$ . Note that the same experiment was carried out in Ref. [14] via the use of H. The values of the relative error, obtained through the 1st-level H-WT, are shown, as black dots, versus the values of  $N$ , reported on the abscissa axis. For each value of  $N$ , the values of the relative error obtained via the 2nd-level H-WT, with  $M \in [3, N - 1]$ , are also plotted and, for the sake of clarity, are joined with lines of different color each of them, which corresponds to a different value of  $N$ , departing from  $N$  itself. This can be noted from the figure, where it is immediately seen how the higher the  $N$ , the longer the corresponding coloured “leg” is. From a first look to the figure, it appears that the relative error, obtained with both the 1st- and the 2nd-level H-WT, is lower bounded. We shall find that all subsequent numerical experiments present the same characteristic. As a first remark, it should be noting that the improvement of the estimate accuracy induced by the 2nd-level H-WT with respect to that obtained via the 1st-level one of the same order appears, at least for values of  $N$  not too large, not to adequately refund the unavoidable increase of the computational complexity required by the application of the 2nd-level transformation. For example, it is seen from Fig. 1 that a relative error of the order of  $10^{-18}$ , achieved through the 2nd-level H-WT with  $N = 11$  and  $M = 8$ , would be reached via a 1st-order H-WT by

letting  $N = 13$ , but with a considerable saving of computational effort. The above example clearly suggests the use of the 2nd-level H-WT only in those cases where the best accuracy attainable via the 1st-level H-WT turns out to be not adequate. This happens, for instance, when the integral is attempted to be evaluated beyond the asymptotic realm. To put into evidence this aspect, Figure 2 shows the same as in Fig. 1, but for a decreasing sequence of values of  $F$ , namely 14 (a), 10 (b), 6 (c), and 2 (d). In particular, in Fig. 2(d), where the Airy function argument is located at a distance  $\simeq 1$  from the origin of the complex plane, the 1st-level H-WT provides a best error of the order of  $10^{-4}$ , achieved for  $N = 4$ . Higher accuracies are not allowed because the information gained at the first H stage turns out to be no longer sufficient to generate WT-resummable sequences. The 2nd-level H-WT, on the other hand, provides a best error of the order of  $10^{-10}$ , which is attained for  $(N, M) = (15, 11)$ . Some intuitive insights about the resummation process associated to the H-WT could be grasped by noting that a lower bounded error is an intrinsic imprint of superasymptotic and hyperasymptotic resummations, whereas it is not generally featured by the application of the WT to alternating factorial divergent series[6]. Accordingly, one should be inclined to think that such an error behavior could be ascribed to the presence of the “regularization” step operated by H on the raw input data. Speaking within a more general context, this should be somewhat related to the possible presence on nonanalytic, nonperturbative correction terms which cannot be grasped simply by resummation processes, but rather require the use of “generalized nonanalytic expansions” [8].

In a second experiment concerning the Airy function, the asymptotic parameter  $F$  is let running within the interval  $[2, 4]$  and, for each value of  $F$ , an exhaustive search of the optimal values of the truncations  $N$  and  $(N, M)$ , which minimize the 1st- and 2nd-level relative errors, respectively, is operated. The results are shown in Fig. 3, where the optimal relative errors obtained via the 1st- (open circles) and the 2nd-level (dots) H-WT are shown as functions of  $F$ . The values of the optimal truncation  $N$  for the 1st-level H-WT are also reported, versus  $F$ , in Fig. 4, while those of  $N$  and  $M$ , for the 2nd-level H-WT, in Fig. 5(a) and (b), respectively. We will come back later on the above results.

In concluding the present section, however, we want to provide a table of explicit values obtained through the use of the 2nd-level H-WT. We choose to evaluate the Airy function for  $F = 2$ , for which the optimal setting of the truncation parameters turns out to be  $(N, M) = (15, 11)$ . The preliminary step is the evaluation, through a simple WT, of the

contribution, to the Airy integral, coming from the saddle  $s_2$ . The result is shown in Table I. Furthermore, the subsequent action of the 2nd-level H-WT on the saddle  $s_1$  is shown in Table II, where the complete estimates of the Airy function provided are reported together with the corresponding values of the truncation  $M \in [3, 14]$ , with  $N = 15$ .

## B. Instanton integral

The second numerical experiment concerns the evaluation of the instanton integral

$$\mathcal{N}(k) = k^{1/2} \int_{-\infty}^{+\infty} \exp[-k(s^2 - 1)^2] ds, \quad (32)$$

with  $k > 0$ , already considered in Ref. [22] as a simplified prototype for the modeling of instanton tunneling between symmetric double wells. It was shown in Ref. [1] that the integral in Eq. (32) can be written as[1]

$$\mathcal{N}(k) = 2 k^{1/2} \operatorname{Re} \{ \mathcal{I}(k) \}, \quad (33)$$

where, by referring to Eq. (1),  $g(s) = 1$ ,  $f(s) = (s^2 - 1)^2$ , and where  $\mathcal{C}$  is the steepest descent path connecting the points  $-\infty$  and  $+\infty$  via the lines  $\operatorname{Im}\{s\} \leq 0$  and  $\operatorname{Re}\{s\} \geq 0$ . The complete saddle topology, as well as the expressions of the expanding coefficients associated to all saddles have been described in Ref. [1]. In particular, there are three saddles,  $s_1 = -1$ ,  $s_2 = 0$ , and  $s_3 = 1$ , with  $\mathcal{A}_1 = \{2\}$ ,  $\mathcal{A}_2 = \{1, 3\}$ , and  $\mathcal{A}_3 = \{2\}$ . The saddles involved in the evaluation of  $\mathcal{I}(k)$  are  $s_2$  and  $s_3$ , but only the latter requires a H-WT treatment, since the associated singulant is  $F_{32} = 1 > 0$ , and the corresponding asymptotic series turns out to be nonalternating. Furthermore,  $\gamma_{12} = 1$ ,  $\gamma_{21} = \gamma_{23} = 0$ , and  $\gamma_{32} = 1$ , while we recall that the integral in Eq. (32) can be expressed in closed form via

$$\mathcal{N}(k) = \frac{\pi \sqrt{k}}{2} \exp(-k/2) \left[ I_{-1/4} \left( \frac{k}{2} \right) + I_{1/4} \left( \frac{k}{2} \right) \right], \quad (34)$$

where  $I_n(\cdot)$  denotes the  $n$ th-order modified Bessel function of the first kind. The first experiment concerns the evaluation of  $\mathcal{N}(1/2)$  via the 1st- and the 2nd-level H-WT. In Fig. 6 it is seen how the 2nd-level relative error is bounded, with a minimum value of the order of  $10^{-3}$ , achieved for  $(N, M) = (6, 5)$ . On the opposite, the 1st-level H-WT turns out to be completely inadequate to provide a reasonably accurate estimate of the function, due to the very low value of  $k$ . The searching for optimal values has also been carried out in

the present case, but using, as the varying asymptotic parameter,  $k \in [1/2, 3]$ , i.e., where the 1st-order H-WT displays the worst results in terms of accuracy, as shown in Fig. 2a of Ref. [1]. The error values are shown in Fig. 7, versus  $k$ , while the optimal settings of  $N$  and of  $(N, M)$  are plotted, against  $k$ , in Fig. 8 and 9, respectively.

It is worth now comparing the results pertinent to the Airy and the  $\mathcal{N}(k)$  functions. What we are going to show can seem at first sight somewhat surprising, but gives a possible first hint toward the understanding of the H-WT mechanisms. For simplicity we shall refer to the 1st-level transformation, but the results will apply also to higher-order levels. In Fig. 10, the values of the relative error obtained for the Airy function (dots) and for the instanton function (solid curve) are plotted, versus  $N$ , when the values of the parameter  $F$  and the parameter  $k$  are numerically equal. In particular, figure (a) corresponds to  $k = F = 3$ , (b) to 7, (c) to 12, and (d) to 20. It is clearly seen that the behavior of the relative error follows basically the same law. To give a possible explanation of this, in Fig. 11 a pictorial representation of the complete saddle network and the complex integration path involved in the evaluation of the Airy (a) and of the instanton (b) functions is plotted. In both pictures, the black dot denotes the saddle for which the H-WT is required. Although the two saddle distributions are clearly different, they present some common features that, together with Eq. (11), are enough to justify what happens in Fig. 10. Each of the “black” saddles is adjacent to a single saddle. For the Airy function  $s_1$  is adjacent to  $s_2$ , while for the instanton function  $s_3$  is adjacent to  $s_2$ . The values of the corresponding singulants are  $F$  and 1, respectively. The use of the resurgence relation in Eq. (8) now gives, for the two “black” saddles,

$$T_r^{(1)} \propto \frac{(r-1)!}{F^r}, \quad (35)$$

for the Airy function and

$$T_r^{(3)} \propto \frac{(r-1)!}{k^r}, \quad (36)$$

for the instanton function. From the above equation it is seen that the behavior of the expanding coefficients follows the same asymptotic law as soon as  $F = k$ . At the same time, however, the above equality guarantees that also the asymptotic laws for the expanding coefficients corresponding to the adjacent saddles is identical. In fact, for the Airy function the saddle adjacent to  $s_2$  is  $s_1$  itself, with a singulant value of  $-F$ . As far as the instanton function is concerned, the saddles adjacent to  $s_2$  are  $s_1$  and  $s_3$ , but for both of them the

singulant values are -1. Accordingly, the use of Eq. (8), together with the condition  $F = k$ , provides again an equivalence between the asymptotic laws of  $T_r^{(2)}$  for the Airy function and  $T_r^{(2)}$  for the instanton function. Finally, on using Eq. (11) it is not difficult to convince that the retrieving process is the same for the two functions at the 1st-level[23]. Leaving a deeper understanding of this phenomenon to future investigations, it is here worthwhile to point out how an immediate consequence of the above described “topological equivalence” could be the restriction of the study of the H-WT retrieving performances to a few classes of prototype test cases.

### C. Swallowtail diffraction catastrophe

As a last numerical experiment we consider asymptotic evaluations of the so-called swallowtail diffraction catastrophe [16, 24, 25, 26], which is defined through the following integral:

$$S(x, y, z) = \int_{\mathcal{C}} \exp \left[ i \left( \frac{s^5}{5} + x \frac{s^3}{3} + y \frac{s^2}{2} + zs \right) \right] ds, \quad (37)$$

which is of the form given in Eq. (1) with  $g(s) = 1$ ,  $f(s) = -i(s^5/5 + xs^3/3 + ys^2/2 + zs)$ , and  $k = 1$ . The integration path  $\mathcal{C}$  can be thought of as the union of steepest descent paths approaching, for  $|s| \gg 1$ , the directions  $\varphi = (2n + 1/2)\pi/5$ , with  $n = 0, 1, \dots, 4$ . Although a systematic treatment of the swallowtail asymptotics, along the general classical rules recalled in Sec. II A, can be derived by paralleling the analysis carried out, for the Pearcey function, in Ref. [15], up to our knowledge it is not present in the current literature. As shown in appendix C, all expanding coefficients  $T_r^{(n)}$  are given by

$$T_r^{(n)} = \frac{(5i)^{r+1/2} (r - 1/2)!}{(10s_n^3 + 5s_n x + 5y/2)^{5r/3+1/2}} B_{2r}^{(r+1/2)}(\alpha, \beta), \quad (38)$$

where

$$\alpha = \frac{5s_n}{(10s_n^3 + 5s_n x + 5y/2)^{1/3}}, \quad (39)$$

$$\beta = \frac{10s_n^2 + 5x/3}{(10s_n^3 + 5s_n x + 5y/2)^{2/3}},$$

and where the polynomials  $B_n^{(\lambda)}(u, v)$  are defined via the generating function formula

$$\sum_{n=0}^{\infty} t^n B_n^{(\lambda)}(u, v) = \frac{1}{(t^3 + ut^2 + vt + 1)^\lambda}. \quad (40)$$



It is not difficult to prove that Eq. (40) allows the numerical evaluation of the polynomials  $B_n^{(\lambda)}(u, v)$  to be efficiently performed via the use of the following recurrence rule, whose derivation is outlined in Appendix D:

$$\begin{aligned} nB_n^{(\lambda)} &= -(n-3+3\lambda) B_{n-3}^{(\lambda)} - u(n-2+2\lambda) B_{n-2}^{(\lambda)} \\ &\quad - v(n-1+\lambda) B_{n-1}^{(\lambda)}, \end{aligned} \tag{41}$$

with the triggering values  $B_0^{(\lambda)}(u, v) = 1$ ,  $B_1^{(\lambda)}(u, v) = -\lambda v$ , and  $B_2^{(\lambda)}(u, v) = -u\lambda + v^2\lambda(\lambda + 1)/2$ .

The numerical experiments we are going to illustrate concern asymptotic evaluations of  $S(x, y, z)$  at points belonging to the corresponding Stokes set, which has been extensively studied in Ref. [5] (see, in particular, Fig. 3 of this reference). Accordingly, the triplets  $(x, y, z)$  have been chosen following the prescriptions given in Ref. [5], in order to investigate points at the intersection between the Stokes surface and the plane  $x = 0$ , along the branch corresponding to  $y > 0$  and  $z > 0$ . This leads to triplets of the form  $(x, y, z) = (0, \kappa^{3/2}, \kappa^2 \times 0.23012\dots)$ , with  $\kappa$  being a positive parameter[5]. We start by considering the case  $\kappa = 2$ . The saddle topology is constituted by four saddles, which are listed below together with the corresponding list of adjacent ones:

$$\begin{aligned} s_1 &= 0.8062\dots - i 1.2357\dots, & \mathcal{A}_1 &= \{4\}, \\ s_2 &= s_1^*, & \mathcal{A}_2 &= \{4\}, \\ s_3 &= -1.2828\dots, & \mathcal{A}_3 &= \{4\}, \\ s_4 &= -0.3296\dots, & \mathcal{A}_4 &= \{1, 2, 3\}, \end{aligned} \tag{42}$$

with the orientation matrix being

$$\{\gamma_{nm}\} = \begin{bmatrix} \cdot & \cdot & \cdot & 1 \\ \cdot & \cdot & \cdot & 0 \\ \cdot & \cdot & \cdot & 0 \\ 0 & 1 & 1 & \cdot \end{bmatrix}, \tag{43}$$

where the values of  $\gamma_{nm}$  which are not relevant for the present experiment have been replaced by dots. Three of the four saddles, namely  $s_2$ ,  $s_3$  and  $s_4$ , do contribute to the integral. In

particular, the integration path consists in the union of three steepest-descent arcs, the first connecting the points  $\infty \exp(i9\pi/10)$  and  $\infty \exp(i13\pi/10)$  passing through  $s_3$ , the second connecting the point  $\infty \exp(i13\pi/10)$  to the saddle  $s_2$ , passing through  $s_4$ , and the third connecting the saddle  $s_2$  to the point  $\infty \exp(i\pi/10)$ . Accordingly, the Stokes phenomenon occurs via the so-called *saddle connection* between saddles  $s_4$  and  $s_2$ [5]. A pictorial representation of the topology above described is given, for the reader convenience, in Fig. 12.

Before showing the numerical results about the performances of the 1st- and the 2nd-level H-WT, it is worth giving some details about the way the saddle topology of the swallowtail integral influences the retrieving capabilities of the WT. We refer, in particular, to the contribution, to the swallowtail integral, of  $s_3$  and  $s_4$ . As far as the former is concerned, since there is only one adjacent saddle,  $s_4$ , due to the fact that the corresponding singulant  $F_{34} = i0.602168\dots$  is purely imaginary, it turns out that  $T_r^{(3)} \propto (-i)^r (r-1)!/|F_{34}|^r$ , thus allowing the WT to operate the resummation. Similar considerations can be done for the contributive saddle  $s_2$ . The situation is somewhat different for the saddle  $s_4$ , which is connected to  $s_2$ . In fact, from the above described topology, it turns out that the adjacent saddle  $s_3$  is dominant, i.e., presents the minimum value of  $|F_{4,m}|$ , with  $m \in \mathcal{A}_4$ . Accordingly, one should conclude also for  $T_r^{(4)}$  an asymptotic “factorial divided by power” law, similar to that corresponding to  $T_r^{(3)}$  and, due to the fact that  $F_{4,3} = -i0.602168\dots$ , one should expect the WT to be able in resumming the corresponding asymptotic series. But this, on the contrary, does not happen, because of the presence of the other two, nondominant, saddles  $s_1$  and  $s_2$ , symmetrically placed in the complex singulant space. This can be explained by expliciting Eq. (8) as

$$T_r^{(4)} \approx \frac{(r-1)!}{2\pi i} \left[ -\frac{T_0^{(3)}}{F_{43}^r} + \left( \frac{T_0^{(1)}}{F_{41}^r} - \frac{T_0^{(2)}}{F_{42}^r} \right) \right], \quad (44)$$

where  $T_0^{(2)} = i[T_0^{(1)}]^*$ . This example shows how the divergent asymptotic series generated on Stokes sets do not necessarily display a strictly nonalternating sign pattern as, for example, happened for the Airy function, but rather how the asymptotic behavior of their single terms can display more complex patterns, depending on the whole saddle topology. Figure 13 shows the relative errors obtained through the 1st- and the 2nd-level H-WTs in the case of swallowtail evaluation across the Stokes set defined above, when  $\kappa = 2$ . As for Figs. 1, 2, and 6, the errors are plotted versus the parameters  $N$  and  $M$ . In this case their optimal

values turn out to be  $N = 4$  (for the 1st-level) and  $(N, M) = (7, 6)$  (for the 2nd-level), with corresponding error values of  $2 \cdot 10^{-3}$  and  $5 \cdot 10^{-5}$ , respectively, evaluated with respect to the “exact” value of  $S(0, 2.8284\dots, 0.9205\dots)$ , obtained via the method recently proposed in Ref. [27]. Finally, an experiment about optimal resummation of swallowtail functions has been carried out, by using  $\kappa \in [2, 4]$  as the parameter representative of the “asymptoticity” features. The error values are shown, versus  $\kappa$ , in Fig. 14, while the optimal settings of  $N$  and of  $(N, M)$  are plotted, against  $\kappa$ , in Fig. 15 and 16, respectively.

## V. CONCLUSIONS

The H-WT was introduced in Ref. [1] as a powerful and easily implementable refinement of H aimed at allowing the WT to successfully decode those divergent asymptotic series generated through the application of the steepest descent method to saddle point integrals evaluated across Stokes sets, for which their single terms do not display a strictly alternating sign pattern. The scheme proposed in [1] employed the WT only on the asymptotic series generated by the first-stage hyperasymptotic treatment of the corresponding diverging remainder. In the present sequel we reported on the possibility of combining H and the WT to higher orders in H. In particular, the full development of the 2nd-level H-WT has been detailed within the classical framework of H. The results obtained from the application of the 2nd-level H-WT, also in comparison to those obtained via the 1st-level one, on the different types of saddle-point integrals considered, showed how the increase of complexity and computational effort required by the new transformation be adequately refunded, in terms of accuracy of the estimate, particularly when the integrals are evaluated for values of their parameters which are beyond the asymptotic regime, whereas H turns out to be inapplicable and the 1st-order H-WT unavoidably lacks precision. At the same time, however, it should be noted how, for “ordinary” asymptotic evaluations, at least in the cases considered in the present work, the performances of the 1st- and the 2nd-level H-WTs seem to be comparable in terms of the estimate accuracy, against a considerably difference in the computational efforts required by the two transformations.

Although the H-WT has been developed, here and in Ref. [1], with reference to the evaluation of saddle-point integrals of the type in Eq. (1), we believe it could be useful also in dealing with problems of different nature like, for instance, the hyperasymptotic treatment

of a wide class of linear and nonlinear ordinary differential equations, which has been recently considered [28, 29, 30]. The semi-analytical algorithms proposed for the numerical evaluation of the 2nd-level hyperterminants would reveal useful in this perspective.

Before concluding, it is worth pointing out, as an important open problem, the need for an *a priori* algorithm for estimating the values of  $N$  and  $M$  that lead to optimal results. Especially in cases where it is not convenient (or possible) to evaluate the original function, such an algorithm would certainly be of great help to a typical user. Unfortunately, differently from  $H$ , for which the optimal settings of the hyperseries truncations are directly extracted from the singulant values [14, 15], at present it does not seem possible to provide similar information for the  $H$ -WT. The difficulties in giving practical guidelines for the choice of  $N$  and  $(N, M)$  can also be appreciated from the results presented in Sec. IV and especially from Figs. 4, 5, 8, 9, 15, and 16, where it seems quite difficult to obtain general rules for the optimal settings of them. A possible hint, grasped from a quantitative comparison between the results obtained for the Airy and the instanton functions, seems to be given by the strong connection between the  $H$ -WT retrieving performances and the saddle topology associated to the integral under consideration. What we found is that different saddle networks can share a sort of “topological equivalence” property, which is related to the set of the saddles adjacent to that under consideration and to the values of the relevant singulants. If two networks turn out to be equivalent at a certain hyperasymptotic level, this would result in the same computational effort, in terms of relative error, as far as the corresponding  $H$ -WT retrieved estimates are concerned. This, in particular, would imply that the study of the  $H$ -WT retrieving performances could be, in principle, carried out only on a restricted class of prototype functions.

## Acknowledgments

I would like to thank all anonymous reviewers for their constructive criticisms and suggestions. I am also grateful to Turi Maria Spinozzi for his invaluable help during the preparation of the present work.

## APPENDIX A: SECOND-STAGE HYPERASYMPTOTICS

The starting point is again the integral representation of the remainder  $R^{(n)}(k, N)$  given in Eq. (10), where we let

$$T^{(m)}\left(\frac{v}{F_{nm}}\right) = \sum_{r=0}^{M-1} \frac{v^{-r}}{F_{nm}^{-r}} T_r^{(m)} + \sum_{r=M}^{\infty} \frac{v^{-r}}{F_{nm}^{-r}} T_r^{(m)}, \quad (\text{A1})$$

with  $M$  being a *new* truncation order. Substitution of Eq. (A1) into Eq. (10) gives

$$\begin{aligned} R^{(n)}(k, N) &= \frac{(-1)^N}{2\pi i} \sum_{m \in \mathcal{A}_n} (-1)^{\gamma_{nm}} \\ &\times \sum_{r=0}^{M-1} (-1)^r k^{-r} T_r^{(m)} K_{N-r}^{(1)}(-kF_{nm}), \\ &+ \frac{1}{2\pi i} \sum_{m \in \mathcal{A}_n} (-1)^{\gamma_{nm}} \\ &\times \sum_{r=M}^{\infty} \frac{(-1)^{N-r}}{(-kF_{nm})^{N-r}} k^{-r} T_r^{(m)} \int_0^{\infty} du \exp(-u) \frac{u^{N-r-1}}{1 - \frac{u}{kF_{nm}}}. \end{aligned} \quad (\text{A2})$$

On using resurgence, i.e., Eq. (8), on  $T_r^{(m)}$ , namely

$$T_r^{(m)} = \frac{1}{2\pi i} \sum_{h \in \mathcal{A}_m} (-1)^{\gamma_{mh}} \sum_{l=0}^{\infty} \frac{(r-l-1)!}{F_{mh}^{r-l}} T_l^{(h)}, \quad (\text{A3})$$

and

$$(r-l-1)! = \int_0^{\infty} dv \exp(-v) v^{r-l-1}, \quad (\text{A4})$$

after straightforward algebra the second term in Eq. (A2) becomes

$$\begin{aligned} &\left(\frac{1}{2\pi i}\right)^2 \sum_{m \in \mathcal{A}_n} \sum_{h \in \mathcal{A}_m} (-1)^{\gamma_{nm} + \gamma_{mh}} \sum_{l=0}^{\infty} k^{-l} T_l^{(h)} \\ &\times \sum_{r=M}^{\infty} \frac{1}{(kF_{nm})^{N-r}} \frac{1}{(kF_{mh})^{r-l}} \\ &\times \int_0^{\infty} \int_0^{\infty} \frac{du}{u} \frac{dv}{v} \exp(-u-v) \frac{u^{N-r} v^{r-l}}{1 - \frac{u}{kF_{nm}}}, \end{aligned} \quad (\text{A5})$$

or, by interchanging the integral with the  $r$ -sum,

$$\begin{aligned}
& \left( \frac{1}{2\pi i} \right)^2 \sum_{m \in \mathcal{A}_n} \sum_{h \in \mathcal{A}_m} (-1)^{\gamma_{nm} + \gamma_{mh}} \sum_{l=0}^{\infty} k^{-l} T_l^{(h)} \frac{(kF_{mh})^l}{(kF_{nm})^N} \\
& \times \int_0^{\infty} \int_0^{\infty} \frac{du}{u} \frac{dv}{v} \exp(-u - v) \frac{u^N v^{-l}}{1 - \frac{u}{kF_{nm}}} \\
& \times \sum_{r=M}^{\infty} \left( \frac{v}{u} \frac{F_{nm}}{F_{mh}} \right)^r = \\
& \left( \frac{1}{2\pi i} \right)^2 \sum_{m \in \mathcal{A}_n} \sum_{h \in \mathcal{A}_m} (-1)^{\gamma_{nm} + \gamma_{mh}} \sum_{l=0}^{\infty} k^{-l} T_l^{(h)} \frac{(kF_{mh})^l}{(kF_{nm})^N} \\
& \times \int_0^{\infty} \int_0^{\infty} \frac{du}{u} \frac{dv}{v} \exp(-u - v) \frac{u^N v^{-l}}{1 - \frac{u}{kF_{nm}}} \frac{\left( \frac{v}{u} \frac{F_{nm}}{F_{mh}} \right)^M}{1 - \left( \frac{v}{u} \frac{F_{nm}}{F_{mh}} \right)}.
\end{aligned} \tag{A6}$$

Eventually, on making the substitution  $-vF_{nm}/F_{mh} \rightarrow v$ , after some algebra the quantity in Eq. (A6) can be written as

$$\begin{aligned}
& \frac{(-1)^{N+M}}{(2\pi i)^2} \sum_{m \in \mathcal{A}_n} \sum_{h \in \mathcal{A}_m} (-1)^{\gamma_{nm} + \gamma_{mh}} \\
& \times \sum_{l=0}^{\infty} k^{-l} T_l^{(h)} K_{M-l, N-M}^{(2)} \left( -kF_{nm}; -\frac{F_{mh}}{F_{nm}} \right),
\end{aligned} \tag{A7}$$

where the 2nd-level hyperterminant  $K_{n,m}^{(2)}(\beta; \gamma)$ , defined by

$$\begin{aligned}
& K_{n,m}^{(2)}(\beta; \gamma) = \frac{1}{\beta^{n+m}} \\
& \times \int_0^{\infty} \int_0^{\infty} du dv \exp(-u - \gamma v) \frac{u^{m-1} v^{n-1}}{\left( 1 + \frac{u}{\beta} \right) \left( 1 + \frac{v}{u} \right)},
\end{aligned} \tag{A8}$$

has been introduced. Accordingly, the complete expression of the 2nd-level hyperasymptotic expansion is

$$\begin{aligned}
T^{(n)}(k) &= \sum_{r=0}^{N-1} k^{-r} T_r^{(n)} \\
&+ \frac{(-1)^N}{2\pi i} \sum_{m \in \mathcal{A}_n} (-1)^{\gamma_{nm}} \\
&\times \sum_{r=0}^{M-1} (-1)^r k^{-r} T_r^{(m)} K_{N-r}^{(1)}(-kF_{nm}) \\
&+ \frac{(-1)^{N+M}}{(2\pi i)^2} \sum_{m \in \mathcal{A}_n} \sum_{h \in \mathcal{A}_m} (-1)^{\gamma_{nm} + \gamma_{mh}} \\
&\times \sum_{r=0}^{\infty} k^{-r} T_r^{(h)} K_{M-r, N-M}^{(2)} \left( -kF_{nm}; -\frac{F_{mh}}{F_{nm}} \right),
\end{aligned} \tag{A9}$$

which coincides with Eq. (14).

## APPENDIX B: DERIVATION OF THE EXTRA TERM FOR $\beta < 0$

We first recast the double integral in Eq. (15) as follows:

$$\begin{aligned}
K_{n,m}^{(2)}(\beta; \gamma) &= \frac{1}{\beta^{n+m-1}} \int_0^\infty dv \exp(-\gamma v) v^{n-1} \\
&\times \int_0^\infty du \exp(-u) \frac{u^m}{(u+\beta)(u+v)},
\end{aligned} \tag{B1}$$

which, if  $\beta$  were not negative, would take the form

$$\begin{aligned}
K_{n,m}^{(2)}(\beta; \gamma) &= \frac{m!}{\beta^{n+m-1}} \int_0^\infty dv \exp(-\gamma v) v^{n-1} \\
&\times \left[ \frac{\exp(v) E_{m+1}(v) - \exp(\beta) E_{m+1}(\beta)}{\beta - v} \right],
\end{aligned} \tag{B2}$$

where the integrand turns out to be continuous even for real, positive values of  $\beta$ , since

$$\begin{aligned} \lim_{v \rightarrow \beta} \frac{\exp(v)E_{m+1}(v) - \exp(\beta)E_{m+1}(\beta)}{\beta - v} &= \\ &= \frac{1 - \exp(\beta)\beta^m(m + \beta)\Gamma(-m, \beta)}{\beta}. \end{aligned} \quad (\text{B3})$$

If  $\beta < 0$ , Eq. (B1) must be written as

$$\begin{aligned} K_{n,m}^{(2)}(\beta; \gamma) &= \frac{1}{\beta^{n+m-1}} \int_0^\infty dv \exp(-\gamma v) v^{n-1} \\ &\times \mathcal{P} \int_0^\infty du \exp(-u) \frac{u^m}{(u + \beta)(u + v)}, \end{aligned} \quad (\text{B4})$$

where  $\mathcal{P} \int_0^\infty \dots$  denotes the principal part operator. On evaluating the integral in Eq. (B4) we have

$$\begin{aligned} \mathcal{P} \int_0^\infty du \exp(-u) \frac{u^m}{(u + \beta)(u + v)} &= \\ &= m! \left[ \frac{\exp(v)E_{m+1}(v) - \exp(\beta)E_{m+1}(\beta)}{\beta - v} \right] \\ &\quad - i\pi \exp(\beta) \frac{(-\beta)^m}{\beta - v}. \end{aligned} \quad (\text{B5})$$

Finally, the direct substitution of Eq. (B5) into Eq. (B4) leads to the closed-form of the extra term as

$$\begin{aligned} \frac{i\pi \exp(\beta)(-\beta)^n}{\beta^{n+m-1}} \int_0^\infty dv \exp(-\gamma v) \frac{v^{n-1}}{v - \beta} &= \\ &= i\pi (-1)^{n+m-1} (n-1)! \frac{\exp[\beta(1-\gamma)]}{(-\beta)^{n-1}} E_n(-\beta\gamma). \end{aligned} \quad (\text{B6})$$

## APPENDIX C: ASYMPTOTIC COEFFICIENTS $T_r^{(n)}$ FOR THE SWALLOWTAIL FUNCTION

The swallowtail function in Eq. (1) corresponds to let  $g = 1$ ,  $k = 1$ , and  $f(s) = -i(s^5/5 + xs^3/3 + ys^2/2 + zs)$  in Eq. (37). The (four) saddle points  $\{s_n\}$  are solutions of the algebraic equation

$$s^4 + x s^2 + y s + z = 0, \quad (\text{C1})$$



which can be exactly solved by using, for instance, Cardano's formula. The evaluation of the expanding coefficients  $T_r^{(n)}$  requires to evaluate the integral in Eq. (6). The first step is to expand  $f(s) - f_n$  around  $s_n$ , i.e.,

$$\begin{aligned} f(s) - f_n &= \\ &= -i \left[ \frac{s^5 - s_n^5}{5} + x \frac{s^3 - s_n^3}{3} + y \frac{s^2 - s_n^2}{2} + z(s - s_n) \right] = \\ &= \frac{(s - s_n)^2}{5i} P(s), \end{aligned} \quad (C2)$$

where

$$P(s) = s^3 + 2s_n s^2 + \left( 3s_n^2 + \frac{5}{3}x \right) s + \left( 4s_n^3 + \frac{10s_n}{3}x + \frac{5}{2}y \right). \quad (C3)$$

Substitution into Eq. (6) gives

$$\begin{aligned} T_r^{(n)} &= \\ &= \frac{(r - 1/2)! (5i)^{r+1/2}}{2\pi i} \oint_n \frac{ds}{(s - s_n)^{2r+1} [P(s)]^{r+1/2}} = \\ &= \frac{(r - 1/2)! (5i)^{r+1/2}}{(2r)!} \left\{ \frac{d^{2r}}{ds^{2r}} \frac{1}{[P(s)]^{r+1/2}} \right\}_{s=s_n}. \end{aligned} \quad (C4)$$

Equation (C4) can be further simplified by letting  $u = s - s_n$  and then by changing  $u$  into  $t = u/(10s_n^3 + 5s_n x + 5y/2)^{1/3}$ , which yields

$$\begin{aligned} T_r^{(n)} &= \frac{(5i)^{r+1/2} (r - 1/2)!}{(10s_n^3 + 5s_n x + 5y/2)^{5r/3+1/2}} \\ &\times \frac{1}{(2r)!} \left[ \frac{d^{2r}}{dt^{2r}} \frac{1}{(t^3 + \alpha t^2 + \beta t + 1)^{r+1/2}} \right]_{t=0}, \end{aligned} \quad (C5)$$

where

$$\begin{aligned} \alpha &= \frac{5s_n}{(10s_n^3 + 5s_n x + 5y/2)^{1/3}}, \\ \beta &= \frac{10s_n^2 + 5x/3}{(10s_n^3 + 5s_n x + 5y/2)^{2/3}}. \end{aligned} \quad (C6)$$

Note that Eq. (C5) can also be given the alternative following form:

$$T_r^{(n)} = \frac{(5i)^{r+1/2} (r - 1/2)!}{(10s_n^3 + 5s_n x + 5y/2)^{5r/3+1/2}} B_{2r}^{(r+1/2)}(\alpha, \beta), \quad (C7)$$

where the function  $B_\lambda^{(n)}(u, v)$  is defined through

$$\sum_{n=0}^{\infty} t^n B_n^{(\lambda)}(u, v) = \frac{1}{(t^3 + ut^2 + vt + 1)^\lambda}, \quad (\text{C8})$$

which coincides with Eq. (40).

#### APPENDIX D: DERIVATION OF THE RECURRENCE RULE IN EQ. (41)

The starting point is the definition of  $B_n^{(\lambda)}(u, v)$  through the generating function in Eq. (C8) which, once derived with respect to  $t$ , gives

$$\sum_{n=0}^{\infty} t^n n B_n^{(\lambda)}(u, v) = -\lambda \frac{3t^3 + 2ut^2 + vt}{(t^3 + ut^2 + vt + 1)^{\lambda+1}}, \quad (\text{D1})$$

and, by taking Eq. (C8) into account once again, leads to

$$\begin{aligned} (3\lambda t^3 + 2\lambda ut^2 + \lambda vt) \sum_{n=0}^{\infty} t^n B_n^{(\lambda)}(u, v) \\ + (t^3 + ut^2 + vt + 1) \sum_{n=0}^{\infty} t^n n B_n^{(\lambda)}(u, v) = 0. \end{aligned} \quad (\text{D2})$$

By operating the products term by term, by rearranging the series indices, after long but straightforward algebra Eq. (41) follows.

- 
- [1] R. Borghi, “Joint use of the Weniger transformation and hyperasymptotics for accurate asymptotic evaluations of a class of saddle-point integrals,” *Phys. Rev. E* **78**, 026703 (2008).
  - [2] M. Born and E. Wolf, *Principles of Optics*, 7th ed. (Cambridge University Press, Cambridge, 1999).
  - [3] M. V. Berry, “Some quantum-to-classical asymptotics,” in *Les Houches Lecture Series LII*, eds. M.-J. Giannoni, A. Voros, and J. Zinn-Justin, *Chaos and Quantum Physics*, Elsevier North-Holland, Amsterdam, 251-304 (1991).
  - [4] F. J. Wright, “The Stokes set of the cusp diffraction Catastrophe,” *J. Phys. A* **13**, 2913-2928 (1980).
  - [5] M. V. Berry and C. J. Howls, “Stokes surfaces of diffraction catastrophes with codimension three,” *Nonlinearity* **3**, 281-291 (1990).
  - [6] E. J. Weniger, “Nonlinear sequence transformations for the acceleration of convergence and the summation of divergent series,” *Comput. Phys. Rep.* **10**, 189-371 (1989).
  - [7] E. J. Weniger, “Mathematical properties of a new Levin-type sequence transformation introduced by Cizek, Zamastil, and Skala. I. Algebraic theory”, *J. Math. Phys.* **45**, 1209-1246 (2004).
  - [8] For an updated review about methods for decoding diverging series, see for instance E. Caliceti, M. Meyer-Hermann, P. Ribeca, A. Surzhykov, and U. D. Jentschura, “From Useful Algorithms for Slowly Convergent Series to Physical Predictions Based on Divergent Perturbative Expansions,” *Phys. Rep.* **446**, 1-96 (2007). arXiv:0707.1596v1.
  - [9] The  $\delta$ - transformation was introduced in Ref. [31] to derive Padé approximants for some hypergeometric functions, but only in Ref. [6] its usefulness as a powerful generalized resummation and convergence acceleration method was demonstrated.
  - [10] C. Brezinski and M. Redivo Zaglia, *Extrapolation Methods* (North-Holland, Amsterdam, 1991).
  - [11] U. D. Jentschura, P. J. Mohr, G. Soff, and E. J. Weniger, “Convergence acceleration via combined nonlinear-condensation transformations,” *Comput. Phys. Comm.* **116**, 28-54 (1999).
  - [12] D. Jentschura, “Resummation of nonalternating divergent perturbative expansions,” *Phys. Rev. D* **62**, 076001 (2000).

- [13] S. V. Aksenov, M. A. Savageau, U. D. Jentschura, J. Becher, G. Soff, and P. J. Mohr, “Application of the combined nonlinear-condensation transformation to problems in statistical analysis and theoretical physics,” *Comput. Phys. Comm.* **150**, 1-20 (2003).
- [14] M. V. Berry and C. J. Howls, “Hyperasymptotics,” *Proc. R. Soc. A* **430**, 653-668 (1990).
- [15] M. V. Berry and C. J. Howls, “Hyperasymptotics for integrals with saddles,” *Proc. R. Soc. A* **434**, 657-675 (1991).
- [16] M. V. Berry and C. Upstill, “Catastrophe optics: morphologies of caustics and their diffraction patterns,” *Prog. Opt.* **XVIII**, 257-346 (1980).
- [17] I. S. Gradshteyn and I. M. Ryzhik, *Table of Integrals, Series, and Products*, 6th ed., A. Jeffrey and D. Zwillinger, eds. (Academic, 2000).
- [18] A. B. Olde Daalhuis, “Hyperterminants I,” *J. Comput. Appl. Math.* **76**, 255-264 (1996).
- [19] A. B. Olde Daalhuis, “Hyperterminants II,” *J. Comput. Appl. Math.* **89**, 87-95 (1998).
- [20] A. P. Prudnikov, Yu. A. Brychkov, and O. I. Marichev, *Integrals and Series. Vol. III* (Gordon Breach Publisher, New York, 1986).
- [21] J. P. Boyd, “The Devil’s Invention: Asymptotic, Supersymptotic and Hyperasymptotic Series,” *Acta Applicandae Mathematicae* **56**, 1-98 (1999).
- [22] M. V. Berry and C. J. Howls, “Infinity interpreted,” *Phys. World* **6**, 35 - 39, (1993).
- [23] It could be proved that the above “equivalence” between the Airy and the instanton functions keeps its validity also for the 2nd-level H-WT.
- [24] J. N. L. Connor, P. R. Curtis, and D. Farrelly, “The uniform asymptotic swallowtail approximation: practical methods for oscillating integrals with four coalescing saddle points,” *J. Phys. A: Math. Gen.* **17**, 281-310 (1984).
- [25] J. F. Nye, *Natural Focusing and Fine Structures of Light*, (Institute of Physics Publishing, Bristol, 1999).
- [26] J. F. Nye, “Dislocation lines in the swallowtail diffraction catastrophe,” *Proc. Roy. Soc. A* **463**, 343-355 (2007).
- [27] R. Borghi, “On the numerical evaluation of cuspid diffraction catastrophes,” *J. Opt. Soc. Am. A* **25**, 1682-1690 (2008).
- [28] A. B. Olde Daalhuis, “Hyperasymptotics for nonlinear ODEs. I. A Riccati equation,” *Proc. R. Soc. Lond. A* **461**, 2503-2520 (2005).
- [29] A. B. Olde Daalhuis, “Hyperasymptotics for nonlinear ODEs II. The first Painlevé equation

- and a second-order Riccati equation,” Proc. R. Soc. Lond. A **461**, 3005-3021 (2005).
- [30] M. V. Berry and A. Shelankov, “The Aharonov-Bohm wave and the Cornu spiral,” J. Phys. A **32**, L447-L455 (1999).
- [31] A. Sidi, “A new method for deriving Padé approximants for some hypergeometric functions,” J. Comput. Appl. Math. **7**, 37-40 (1981).

## LIST OF TABLES

WT order	Contribution of saddle $s_2$
2	<u>0.02315166515</u> + <u>0.04009986036</u> i
3	<u>0.02303913417</u> + <u>0.03990495099</u> i
4	<u>0.02305968041</u> + <u>0.03994053805</u> i
5	<u>0.02305839073</u> + <u>0.03993830429</u> i
6	<u>0.02305829942</u> + <u>0.03993814613</u> i
7	<u>0.02305830901</u> + <u>0.03993816279</u> i
8	<u>0.02305831068</u> + <u>0.03993816566</u> i
9	<u>0.02305831068</u> + <u>0.03993816562</u> i
10	<u>0.02305831064</u> + <u>0.03993816557</u> i
11	<u>0.02305831064</u> + <u>0.03993816557</u> i
...	...

TABLE I: Values, provided by the WT, of the contribution coming from the saddle  $s_2$  in the evaluation of the Airy function across its Stokes set, when  $F = 2$ .

M	H-WT estimate
3	<u>0.7906105793</u> - <u>0.4032083434</u> i
4	<u>0.7061079570</u> - <u>0.3544207316</u> i
5	<u>0.7018070334</u> - <u>0.3519375922</u> i
6	<u>0.7015955837</u> - <u>0.3518155117</u> i
7	<u>0.7015834126</u> - <u>0.3518084847</u> i
8	<u>0.7015826207</u> - <u>0.3518080275</u> i
9	<u>0.7015825835</u> - <u>0.3518080060</u> i
10	<u>0.7015825939</u> - <u>0.3518080120</u> i
11	<u>0.7015826051</u> - <u>0.3518080185</u> i
12	<u>0.7015826244</u> - <u>0.3518080296</u> i
13	<u>0.7015563466</u> - <u>0.3517928581</u> i
14	<u>0.7015826472</u> - <u>0.3518080428</u> i
exact	0.7015826047 - 0.3518080182 i

TABLE II: Estimates, provided by the 2nd-level H-WT, of the Airy function across its Stokes set, when  $F = 2$ . Note that the truncation parameter  $N$  has been fixed to 15 (corresponding, from Fig. 5, to the optimal setting).

## LIST OF FIGURE CAPTIONS

FIG. 1: Behavior of the relative error, obtained through the 1st-level H-WT (dots), versus the values of  $N$ , which are reported on the abscissa axis. For each value of  $N$ , the values of the relative error obtained via the 2nd-level H-WT, with  $M \in [3, N - 1]$ , are also plotted and, for the sake of clarity, are joined with lines of different color, each of them corresponding to a different value of  $N$ , departing from the abscissa  $N$  itself.

FIG. 2: The same as in Fig. 1, but for  $F = 14$  (a), 10 (b), 6 (c), and 2 (d).

FIG. 3: Behaviors, as functions of  $F \in [2, 4]$ , of the relative errors for the Airy function obtained via the 1st- (open circles) and the 2nd-level (dots) H-WT. Each point has been obtained by carrying out, for a given  $F$ , an exhaustive search for those values of the truncations  $N$  and  $(N, M)$  which minimize the corresponding 1st- and 2nd-level relative errors, respectively.

FIG. 4: Behavior, as a function of  $F$ , of the values of  $N$  corresponding to the optimal setting for the 1st-level H-WT in the experiment of Fig. 3.

FIG. 5: Behavior, as a function of  $F$ , of the values of  $N$  (a) and  $M$  (b) corresponding to the optimal setting for the 2nd-level H-WT in the experiment of Fig. 3.

FIG. 6: The same as in Fig. 1, but for the instanton integral  $\mathcal{N}(1/2)$ .

FIG. 7: Behaviors, as functions of  $k \in [1/2, 3]$ , of the relative errors for the instanton integral  $\mathcal{N}(k)$  obtained via the 1st- (open circles) and the 2nd-level (dots) H-WT. As for the results presented in Fig. 3, each point has been obtained by carrying out, for a given  $k$ , an exhaustive search for those values of the truncations  $N$  and  $(N, M)$  which minimize the corresponding 1st- and 2nd-level relative errors, respectively.



FIG. 8: Behavior, as a function of  $k$ , of the values of  $N$  corresponding to the optimal setting for the 1st-level H-WT in the experiment of Fig. 7.

FIG. 9: Behavior, as a function of  $k$ , of the values of  $N$  (a) and  $M$  (b) corresponding to the optimal setting for the 2nd-level H-WT in the experiment of Fig. 7.

FIG. 10: Behavior of the relative error obtained for the Airy function (dots) and for the instanton function (solid curve) versus  $N$ , for  $F = k = 3$  (a), 7 (b), 12 (c), and 20 (d).

FIG. 11: Pictorial representation of the saddle networks and of the complex integration paths involved in the evaluation of the Airy (a) and of the instanton (b) functions.

FIG. 12: The same as in Fig. 11, but for the evaluation of the swallowtail diffraction catastrophe at the points across the Stokes set given by the triplets  $(x, y, z) = (0, \kappa^{3/2}, \kappa^2 \times 0.23012\dots)$ , with  $\kappa > 0$ .

FIG. 13: The same as in Fig. 1, but for the swallowtail function evaluated across the Stokes set  $(x, y, z) = (0, \kappa^{3/2}, \kappa^2 \times 0.23012\dots)$  with  $\kappa = 2$ .

FIG. 14: Behaviors, as functions of  $\kappa \in [2, 4]$ , of the relative errors for the swallowtail function evaluated across the Stokes set  $(x, y, z) = (0, \kappa^{3/2}, \kappa^2 \times 0.23012\dots)$  obtained via the 1st- (open circles) and the 2nd-level (dots) H-WT. As for the results presented in Fig. 3, each point has been obtained by carrying out, for a given  $k$ , an exhaustive search for those values of the truncations  $N$  and  $(N, M)$  which minimize the corresponding 1st- and 2nd-level relative errors, respectively.

FIG. 15: Behavior, as a function of  $\kappa$ , of the values of  $N$  corresponding to the optimal setting for the 1st-level H-WT in the experiment of Fig. 14.

FIG. 16: Behavior, as a function of  $\kappa$ , of the values of  $N$  (a) and  $M$  (b) corresponding to the optimal setting for the 2nd-level H-WT in the experiment of Fig. 14.

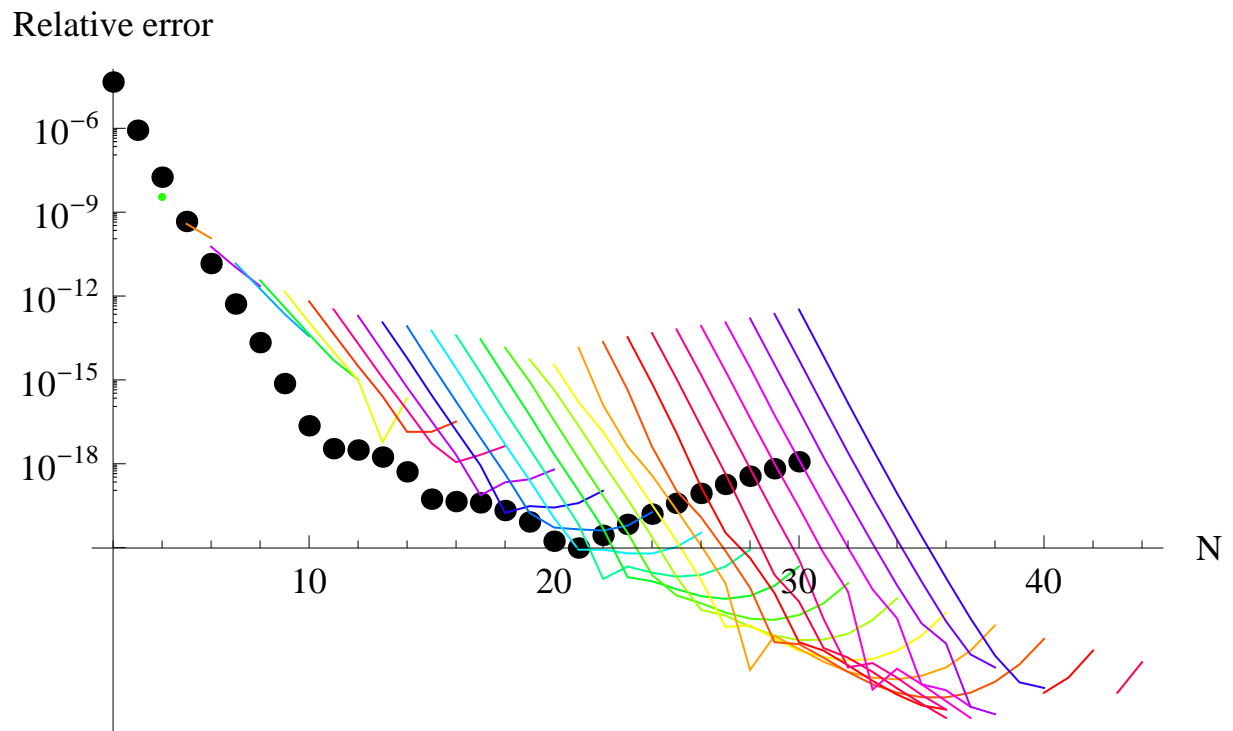


Fig. 1 - R. Borghi

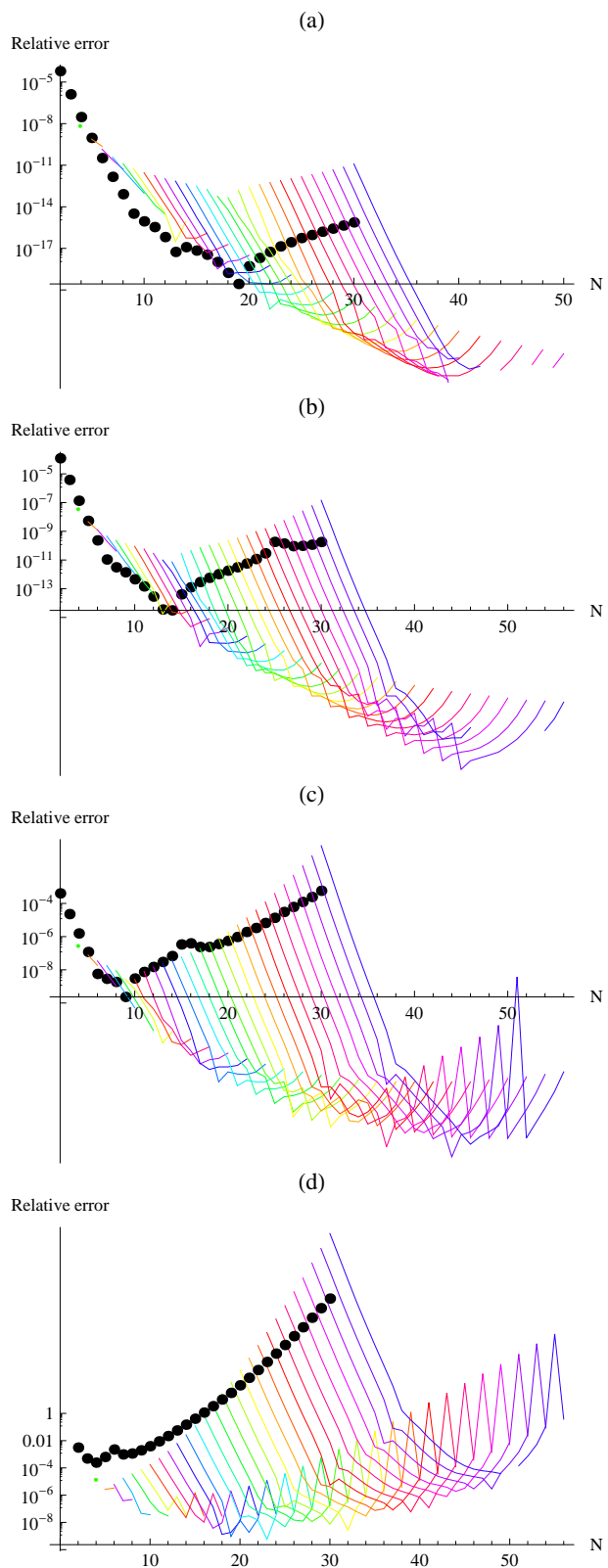


Fig. 2 - R. Borghi

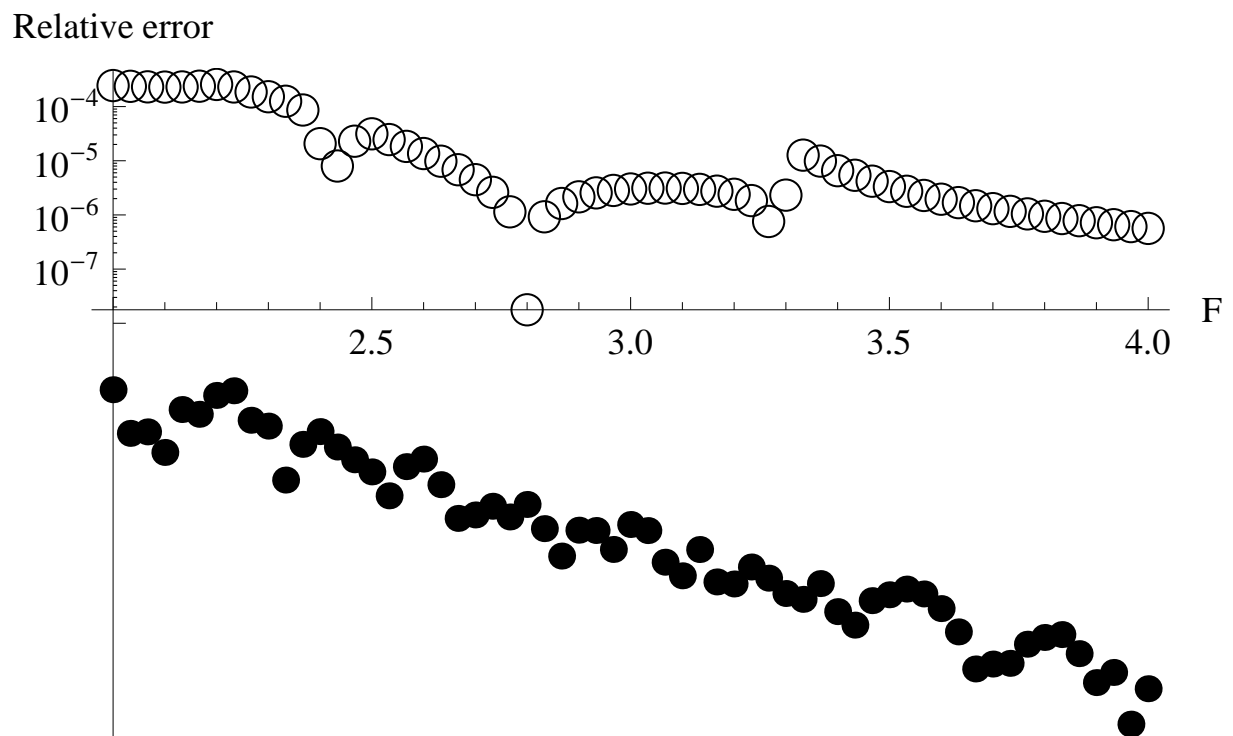


Fig. 3 - R. Borghi

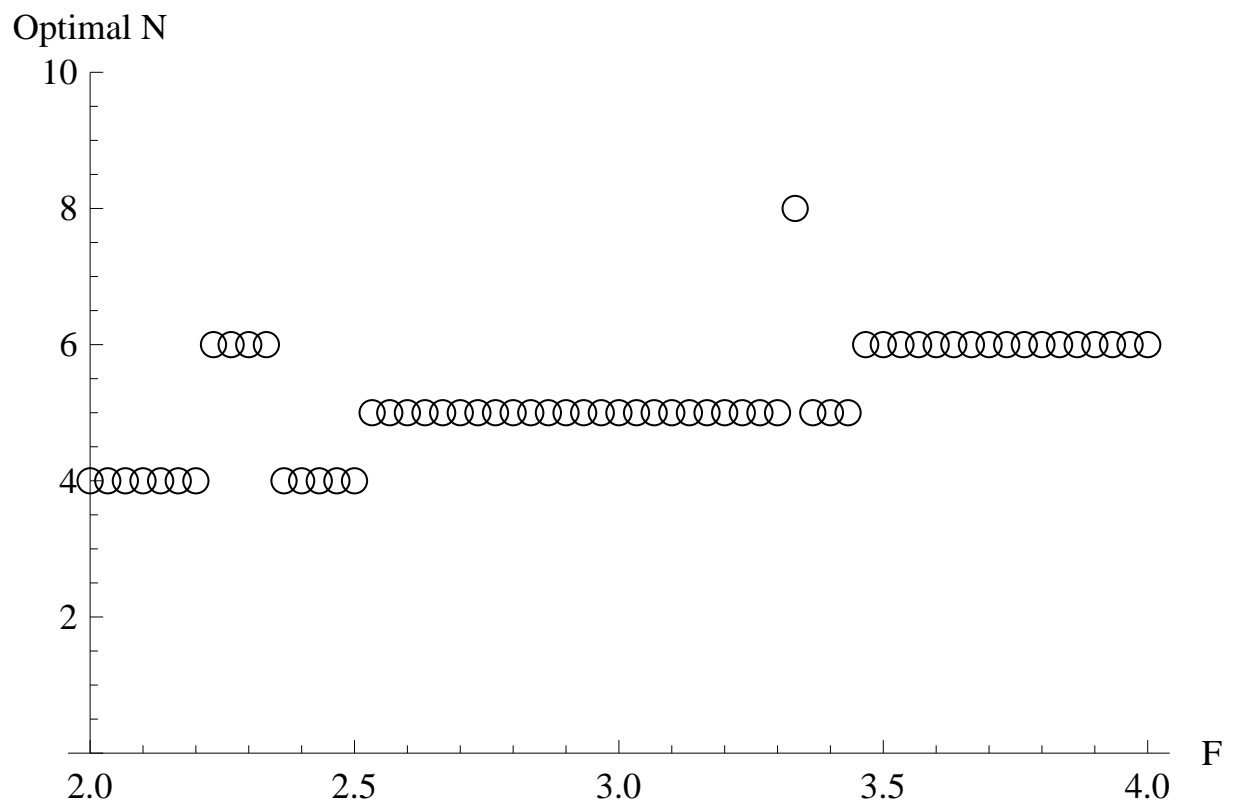


Fig. 4 - R. Borghi

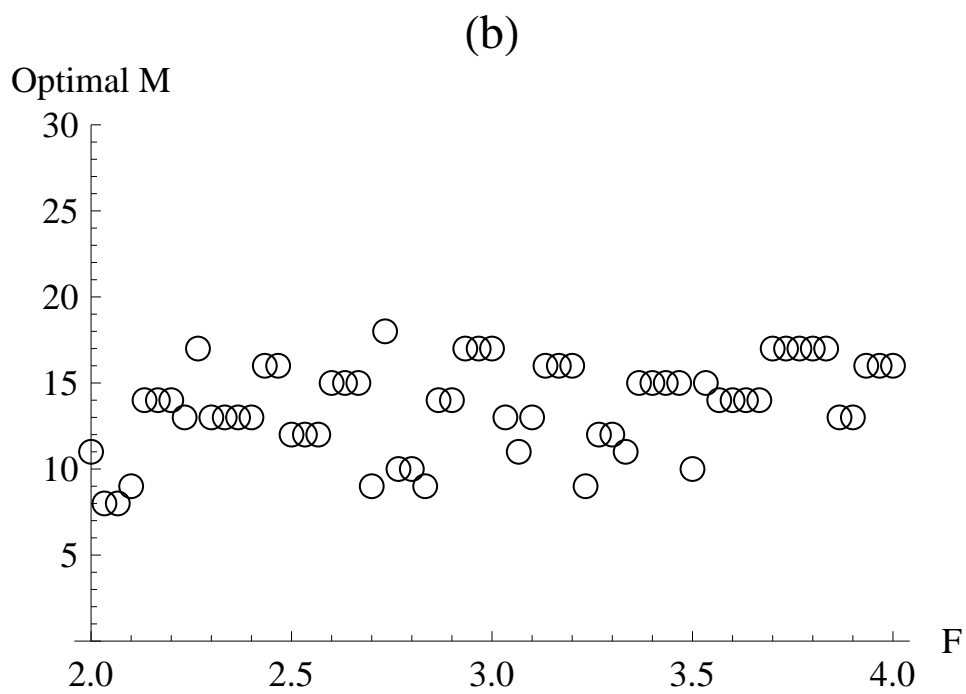
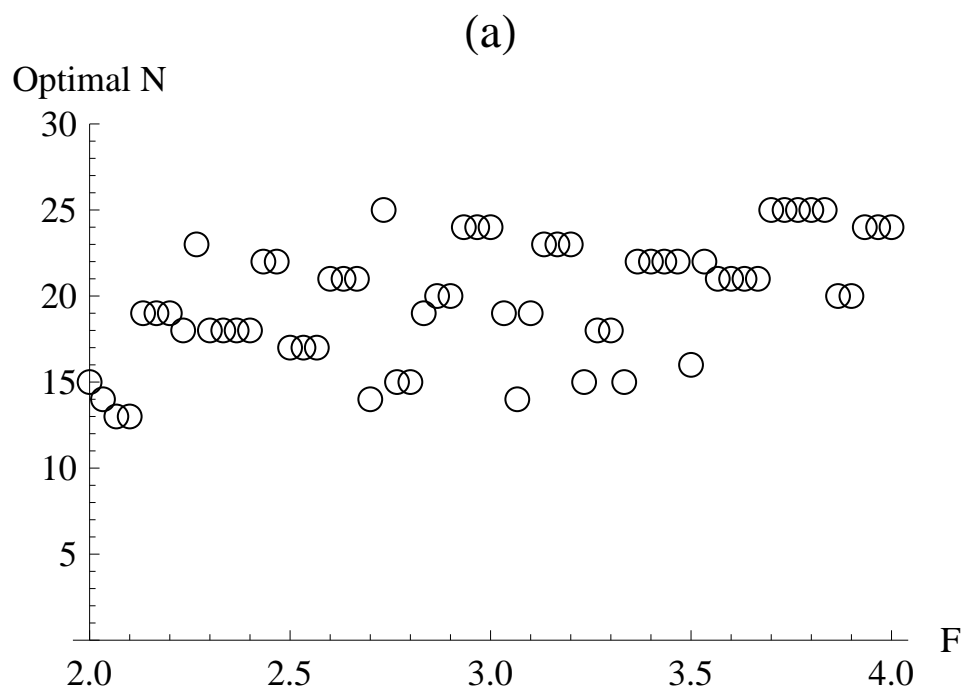


Fig. 5 - R. Borghi

Relative error

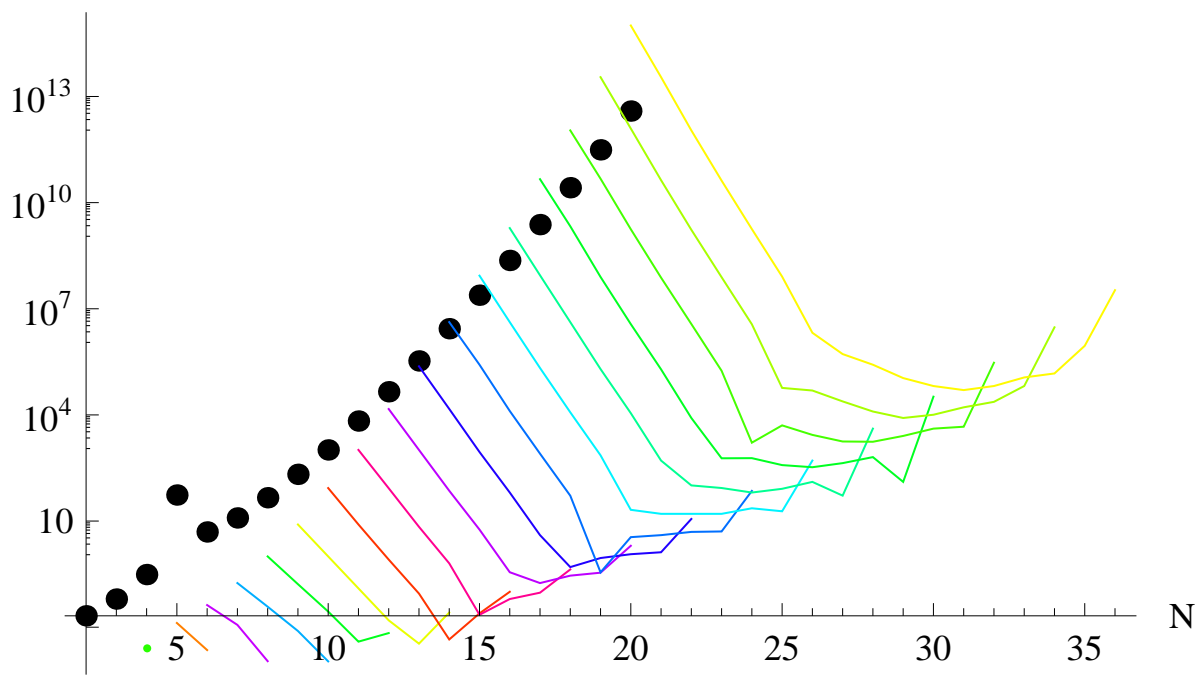


Fig. 6 - R. Borghi

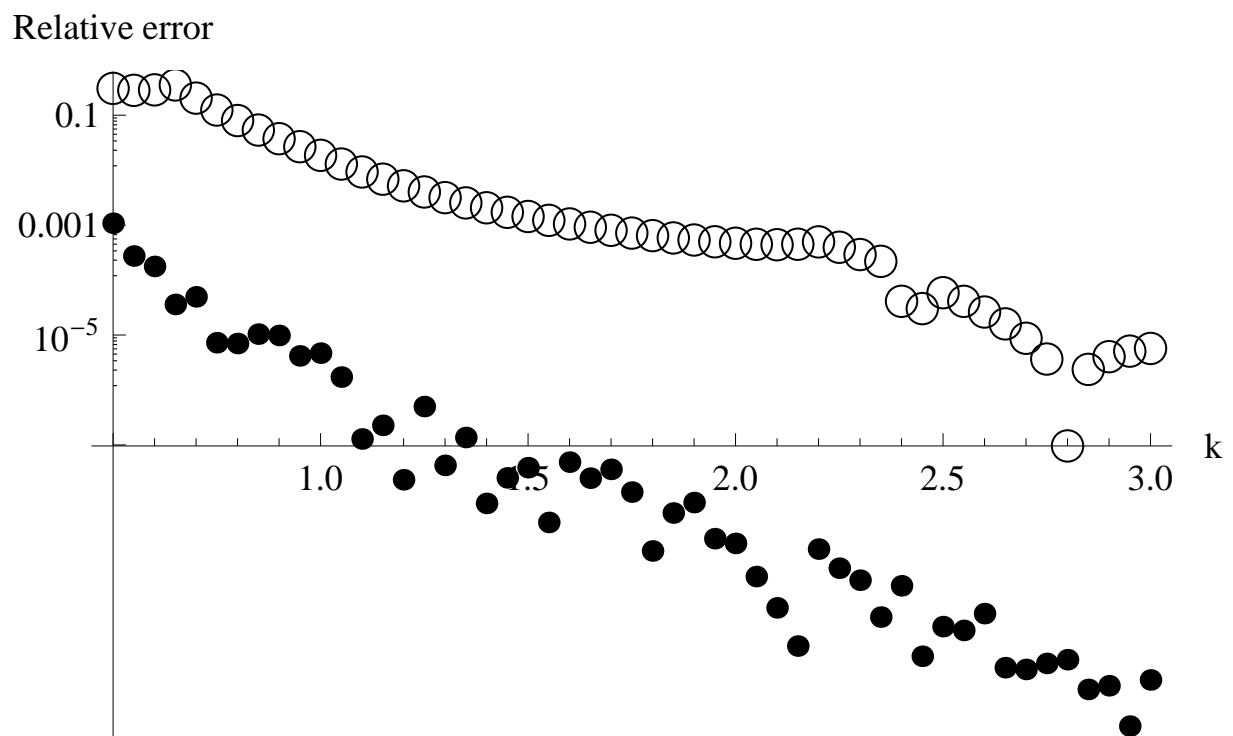


Fig. 7 - R. Borghi



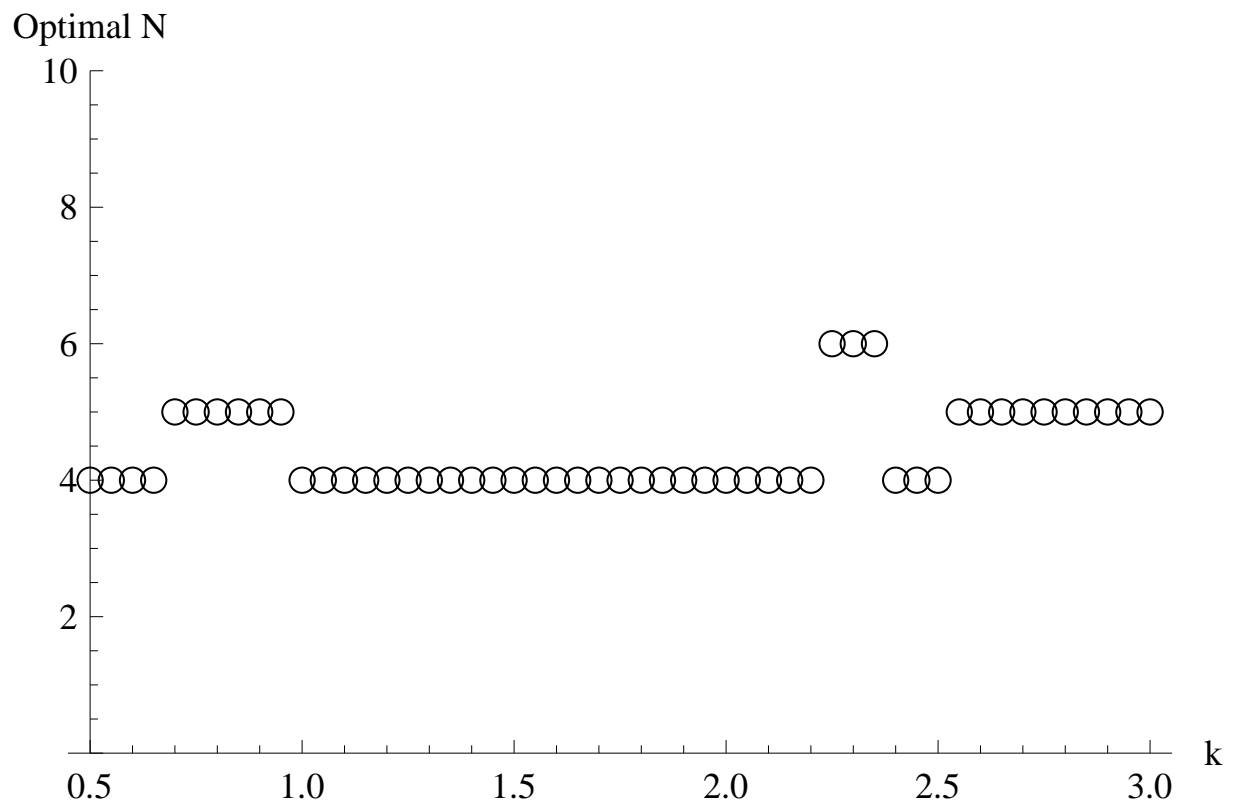


Fig. 8 - R. Borghi

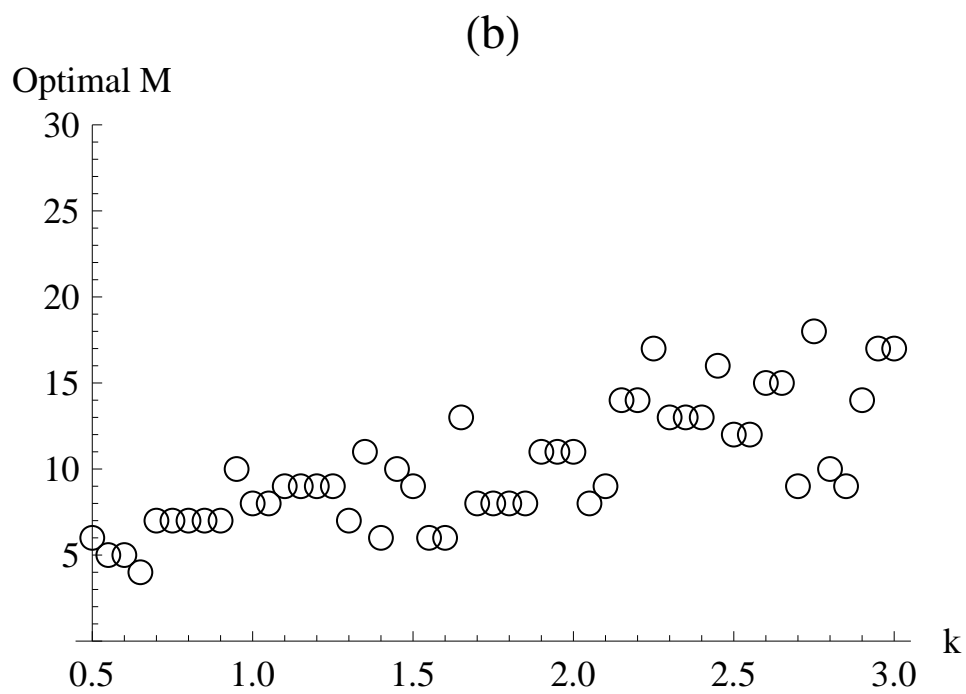
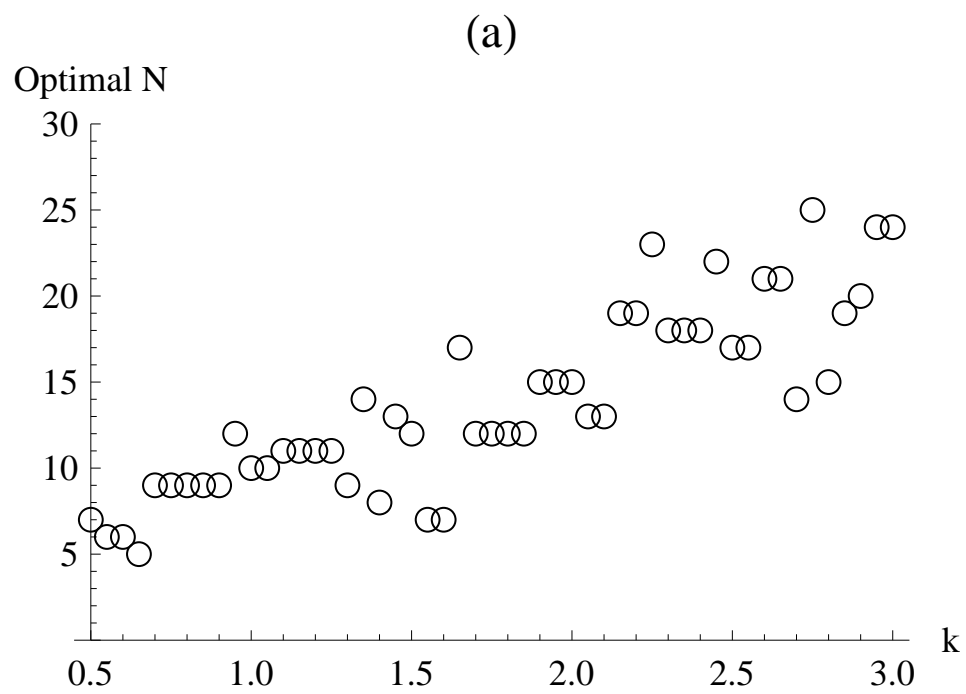


Fig. 9 - R. Borghi

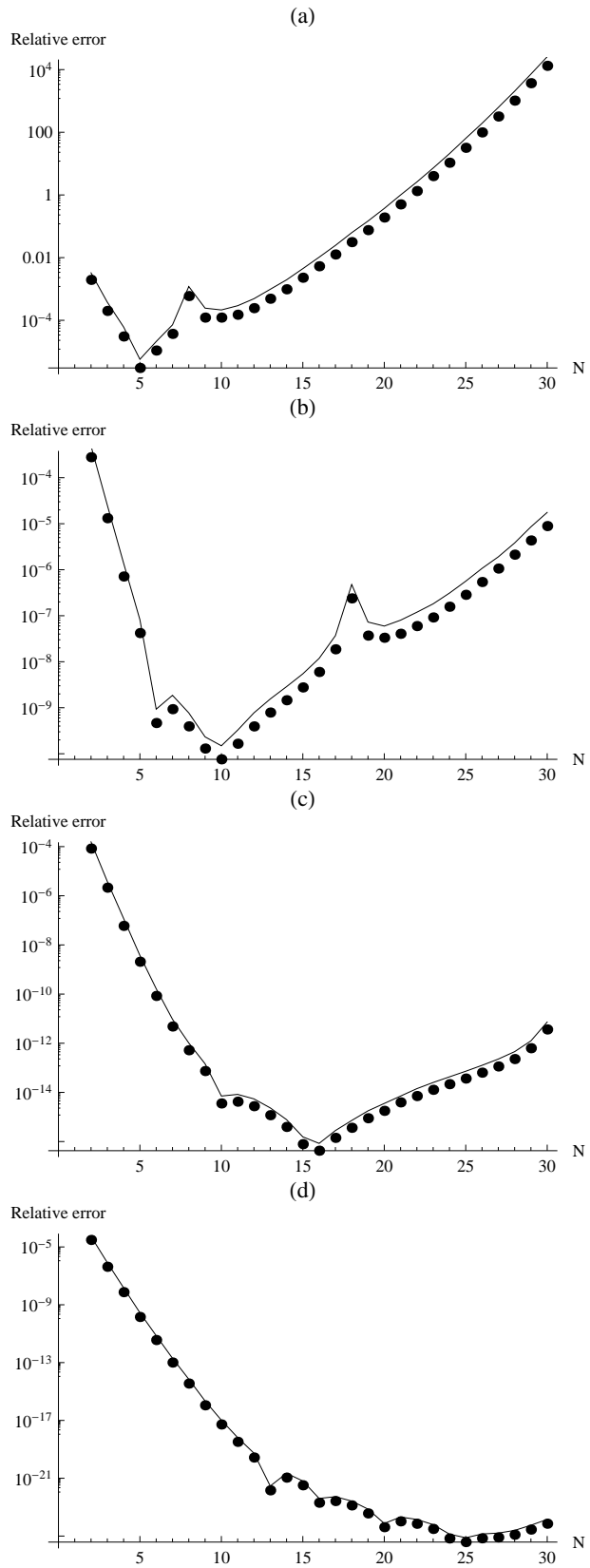
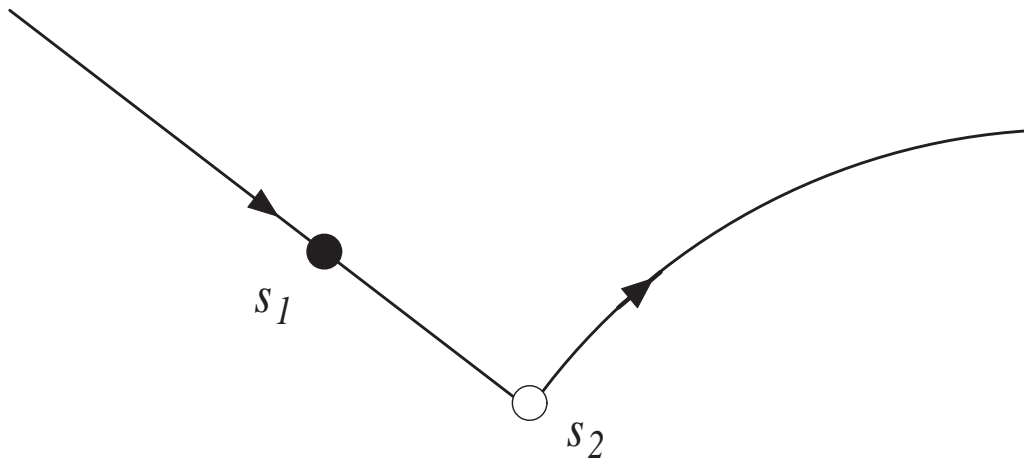


Fig. 10 - R. Borghi

(a)



(b)

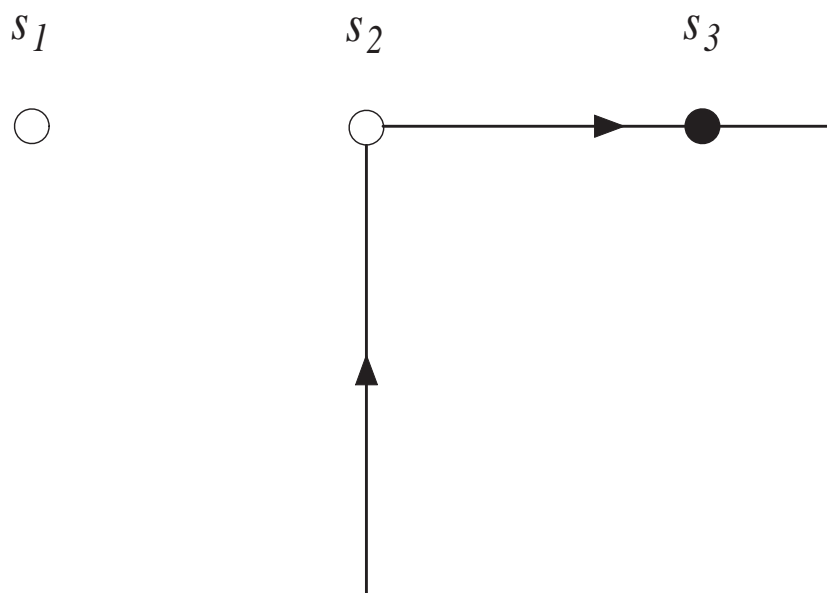


Fig. 11 - R. Borghi

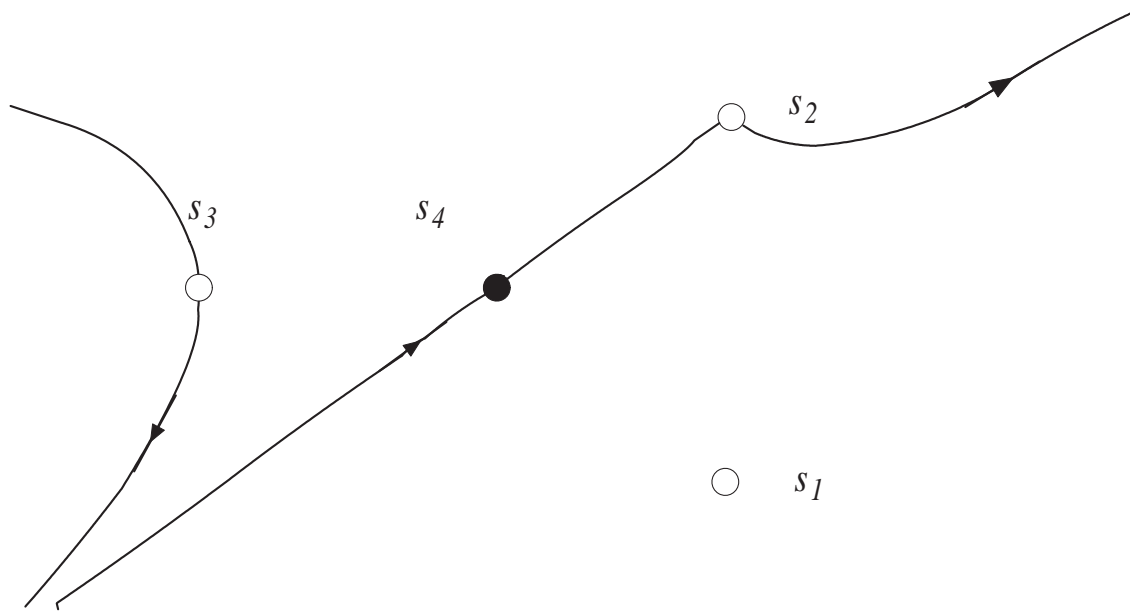


Fig. 12 - R. Borghi

Relative error

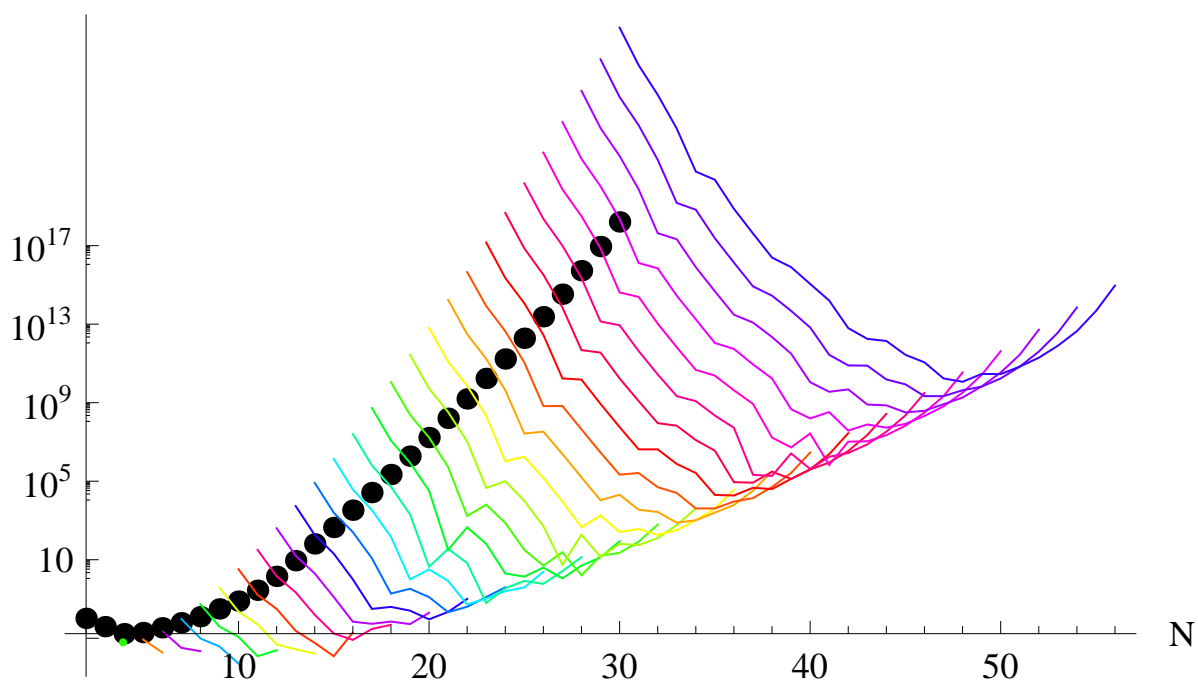


Fig. 13 - R. Borghi

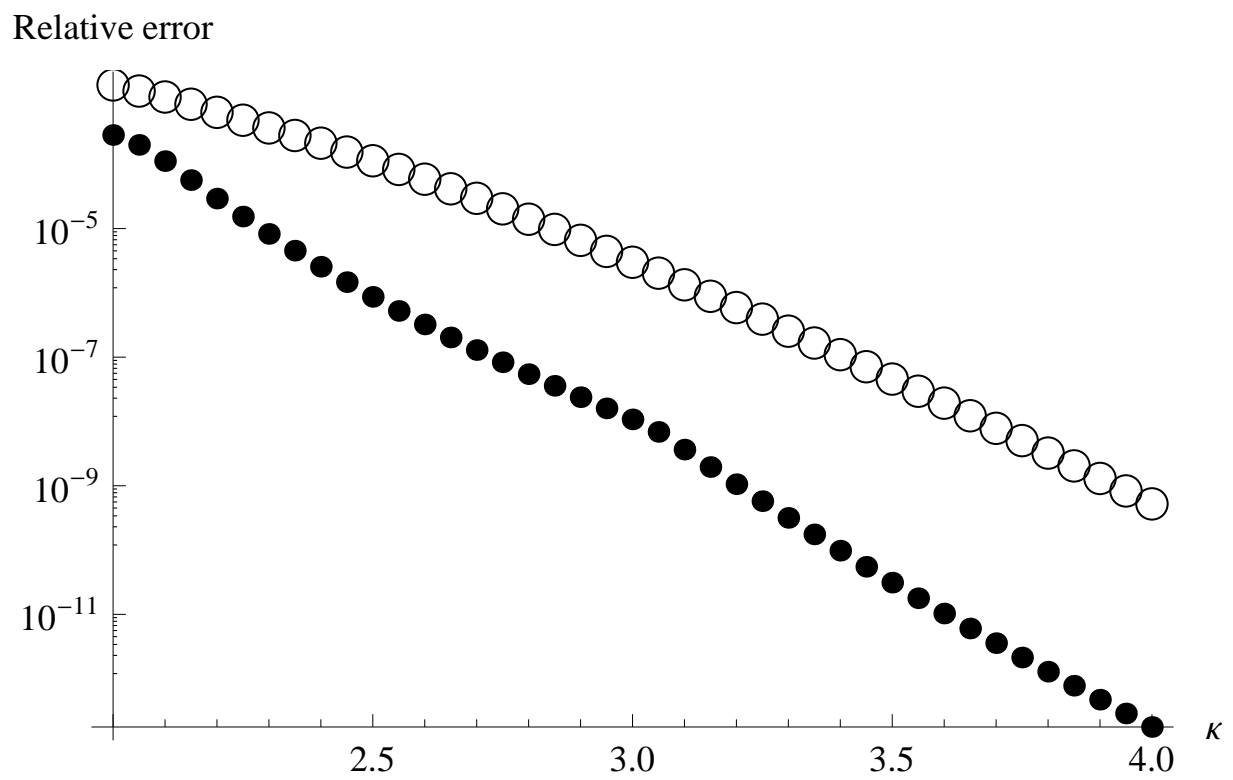


Fig. 14 - R. Borghi

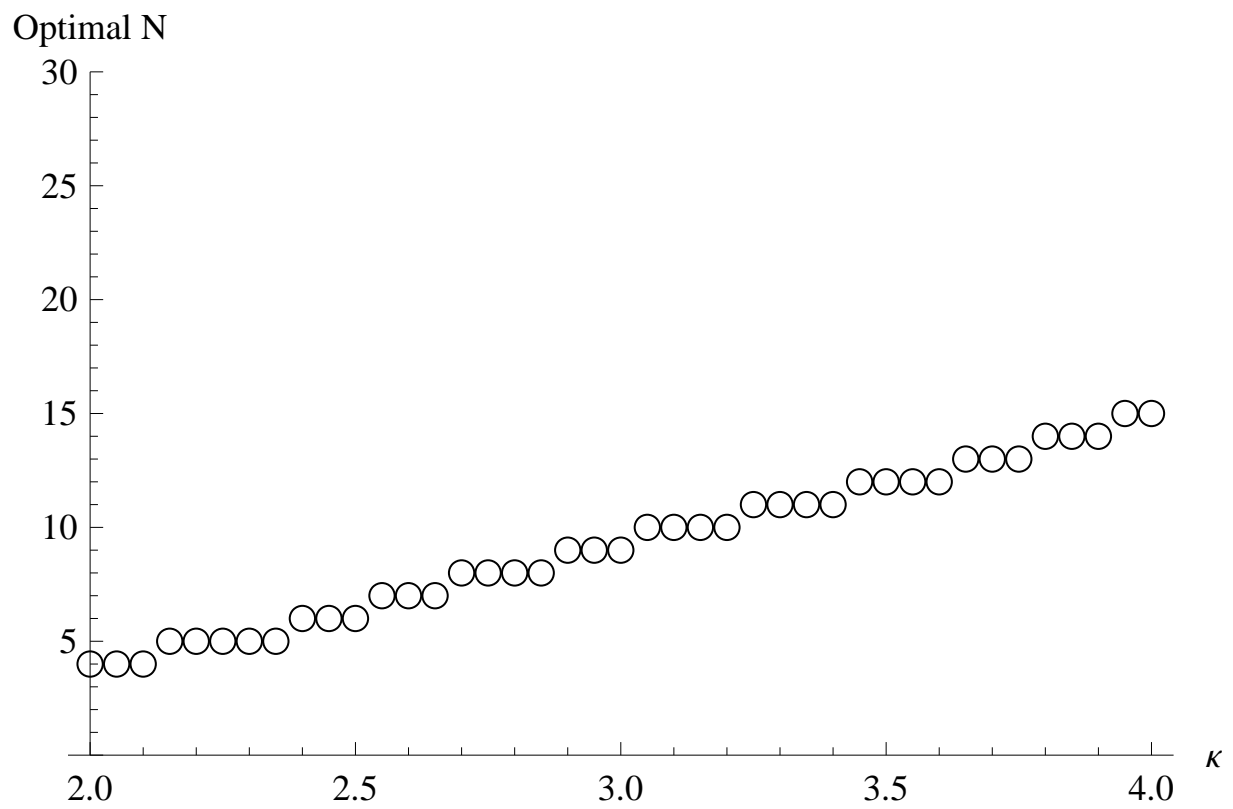


Fig. 15 - R. Borghi



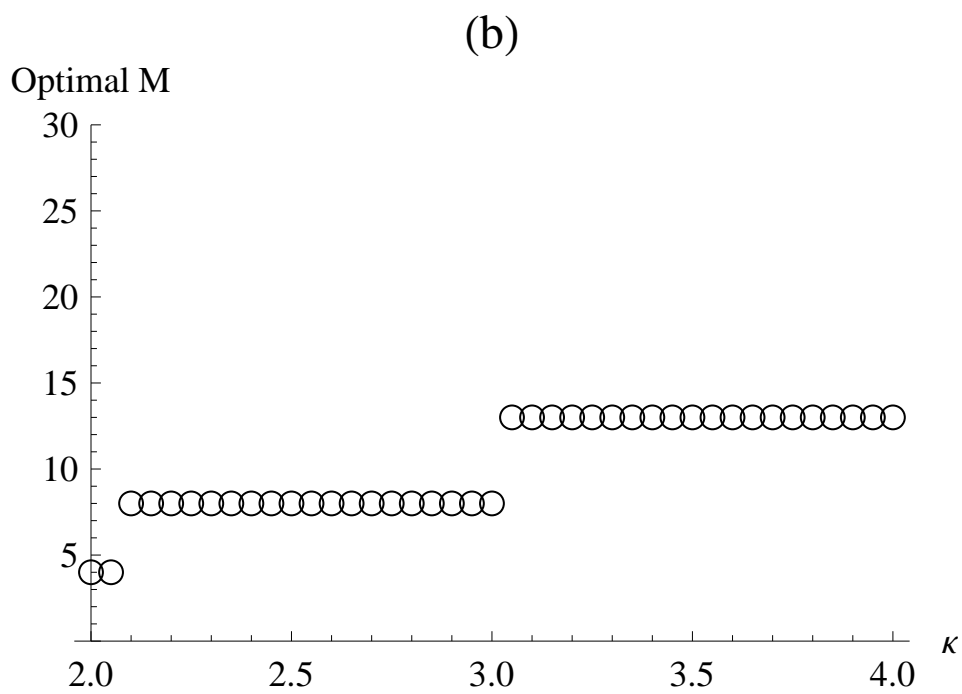
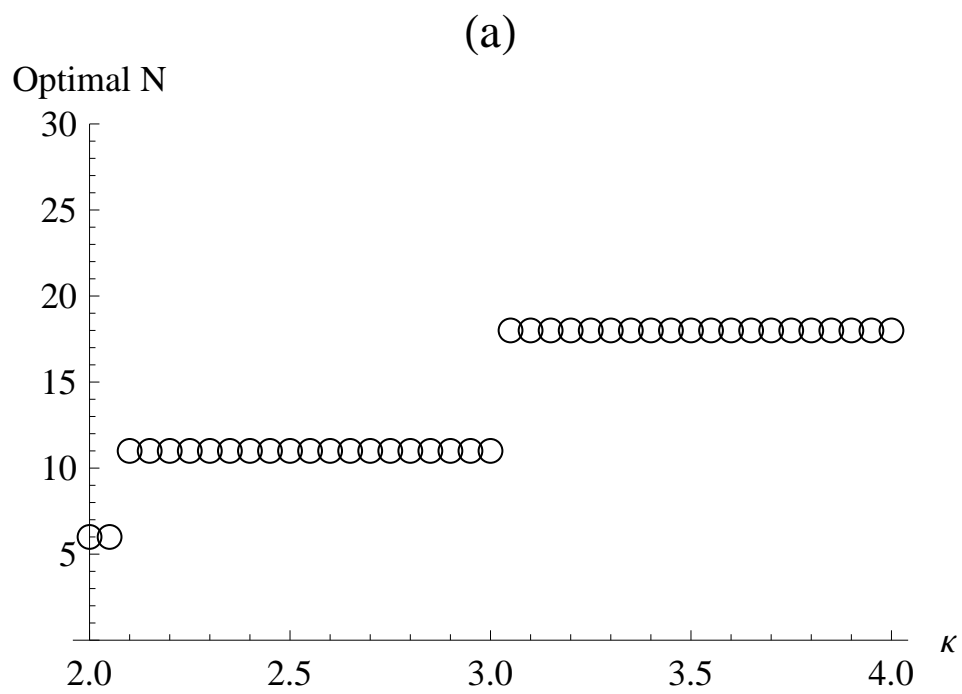


Fig. 16 - R. Borghi